Technical Report-Hydrology Model
Troilus Impact Assessment

Prepared for:

Troilus Gold Corporation
1155 René-Lévesque Boulevard West, Suite 3300,
Montreal, QC H3B 3X7

Prepared by:

BluMetric Environmental Inc.

1500 du Collège Street
Saint-Laurent, QC H4L 5G6

Project Number: 240433
June 2025

Table of Contents

List of Figures

List of Tables

1 Model Description

1.1 Introduction

This technical appendix describes the hydrologic modelling methodology, data inputs, calibration, and climate considerations for the Troilus Project. The modelling, aimed at informing regulatory impact assessment, was performed using HEC-HMS (Hydrologic Engineering Center's Hydrologic Modeling System) version 4.5. Key processes include rainfall-runoff generation using Soil Conservation Service methods, flow routing via kinematic wave, baseflow simulation, and snowmelt modeling. Data from high-resolution topography, climate stations, and field hydrology campaigns were integrated to build and calibrate the model. Calibration results and climate-adjusted scenarios are presented, followed by a discussion of assumptions, limitations, and uncertainties.

1.2 Background

The Local Study Area (LSA) is mainly located in the Natastan watershed of the Rupert River, with some sub-watersheds slightly exceeded in the Broadback River watershed (Map 11.3). Similarly, the majority of the Regional Study Area (RSA) lies within the Rupert River watershed, with a slight overflow into the Broadback River watershed to the southwest (Map 11.4). The region's topography is characterized by gentle slopes. The landscape consists of rocky massifs overlying glacial and fluvioglacial terrain, as well as extensive peatlands and wetlands offering a flattened landscape. The surface of the land consists of a sandy fill three to five metres (m) deep. Beneath this layer, to a depth of around 24 m, is a natural soil deposit composed of clay over volcanic bedrock (Inmet Mining Corporation 1996; Tremblay et al., 1995).

The LSA's hydrographic network consists of a chain of lakes starting with Lac Amont (PE-2) to the southwest, passing through several lakes and bodies of water PE0-63 , as well as lakes of particular interest: Lac D1 (PE9), Lac D2 (PE17), Lac C (PE8), Lac B (PE29), Lac B2 (PE33), Lac B3 (PE36), Lac B4 (PE17), Lac A (PE43), Lac A1 (PE48), Lac A2 (PE50) and Lac Hameçon (PE58), before emptying into Lac Boisfort, located some 10 km north of the ZDP. Lac Boisfort is located within the RSA. It drains a 387 km2 sub-watershed, of which the mine site valley represents 8%. Map 11.4 shows the location of the main water bodies in the RSA.

A watercourse approximately 8.8 km long links Lac A2 (PE50) to Lac Boisfort. The watercourse leading to the outlet of Lake A (PE43) is meandering, with a low flow rate and a width varying from 3 to 5 m depending on the water level. The existing ruisseau Bibou links Lac Amont (PE2) to Lac A (PE43). Part of the existing creek is a historic diversion channel that carries flow around the tailings storage area (TSF), pit 87 and pit J. The existing Bibou Creek (CE2) has a drainage area of 31.2 km^2 at its confluence with Lake A (PE43). Bibou Creek (CE2) has a water depth of between 0.3 m and 1.2 m (WSP, 2024). The portion of the stream currently diverted shows signs of erosion, and is between 5 and 7 m wide. A new detour of Bibou Creek (CE2) is planned, to divert runoff from upstream natural watersheds around the project development area (PDA) (WSP, 2024). Chapter 3 and the Water Management Plan (WSP, 2024) detail the proposed diversion of Bibou Creek (CE2).

1.3 Methodology

A continuous hydrology model was implemented in HEC-HMS 4.5, employing standard hydrological methods suitable for northern watershed conditions. The following components define the modelling approach:

- **Infiltration (Loss) Method – SCS Curve Number (CN):** Rainfall losses to infiltration were estimated using the SCS Curve Number method, an empirical approach relating land cover, soil type, and antecedent moisture to runoff generation. Each sub-basin was assigned to a CN value (30 to 100, dimensionless) corresponding to its dominant land use and soil conditions. A lower CN (e.g. ~60 for undisturbed wood) indicates higher infiltration and storage, whereas a higher CN (e.g. 90+ for impervious or compacted surfaces) produces more direct runoff. Initial abstractions were represented as a fraction of potential retention. This method allowed the model to partition rainfall into runoff and infiltration consistently across the watershed.
- **Runoff Transformation – SCS Unit Hydrograph:** The excess precipitation (after losses) was transformed into runoff hydrographs using the SCS Unit Hydrograph method. This method applies a dimensionless unit hydrograph shape developed by the SCS to predict the time distribution of flow from a design storm. Key parameters include the sub-basin lag time (time to peak), estimated from land slope and flow length. The SCS unit hydrograph provides a reasonable approximation of catchment response in small to medium basins, given the soil and cover conditions.
- **Flow Routing – Kinematic Wave Routing:** For channel and drainage network routing, the model employed kinematic wave routing (KWR). This is a distributed, one-dimensional routing method solving the simplified shallow water equations under the assumption that flow is inertia-less and is driven by gravity and friction (no backwater effects). Channel reaches (e.g. the Bibou Creek) were represented with cross-section, slope, and roughness inputs. Kinematic wave routing propagates the flood wave through each reach, accounting for translation and attenuation of flow. This method is appropriate given the generally mild channel slopes and the need to simulate timing of peaks to downstream points. It was used

to route hydrographs through natural creeks and proposed diversion channels to assess peak flows and water levels. For small reaches and creeks where kinematic wave routing could not be applied, a lumped lag time was assigned in accordance with the WSP (2024) report.

- **Baseflow Estimation – Recession Method:** Continuous baseflow contributions were simulated using the exponential recession method in HEC-HMS. This method assumes baseflow (groundwater discharge to streams) decays exponentially after precipitation events. Each sub-basin was assigned an initial baseflow and a recession constant representing how quickly baseflow recedes. The recession constant was calibrated so that simulated low flows and groundwater contributions matched observed conditions. Essentially, after storm runoff passes, baseflow recedes as $Q_b(t) = Q_{b0}. e^{-kt}$ where Q_{b0} is initial baseflow and k is the decay coefficient. This provided a simple representation of groundwater drainage supporting streamflow between rain events.
- **Snow Accumulation and Melt –Temperature Index Method:** Given the region's significant snowfall, the model incorporated a degree-day (temperature index) algorithm to represent snow processes. Snow accumulation and melt were driven by daily temperature and calibrated parameters: precipitation temperature threshold, base temperature, and the ATI (Accumulation–Temperature Index) coefficient. This approach allowed simulation of both spring melt events and rain-on-snow floods, with the snowpack tracked over winter and spring melt pulses generated in accordance with temperature-driven melt dynamics.
- **Potential Evapotranspiration (PET)- Hamon**: Hamon method, calculates daily PET as a function of mean daily air temperature and daylight hours. The Hamon model coefficient was calibrated to regional conditions and applied across the site for the historical and projection periods.

1.4 Data Sources and Model Inputs

The hydrological model integration relied on multiple data sources to characterize the watershed and climatic inputs. Key data sources and model inputs are as follows:

- **Topography and Sub-Basin Delineation:** 1 m LiDAR-derived DEM sourced from Quebec Government's Ministry of Natural Resources and Forestry https://www.donneesquebec.ca/recherche/dataset/produits-derives-de-base-du-lidar was used to delineate catchment boundaries and drainage networks in GeoHEC-HMS software. Sub-basin boundaries were refined to reflect the actual locations of open pits, stockpiles, and other mining infrastructure.

- **Climate Station Data (ECCC 7091405):** Regional climate data were obtained from the Environment and Climate Change Canada (ECCC) station Chibougamau Chapais A (Station ID 7091405, 49°46′19″N, 74°31′41″W). This station, located ~136 km south of the site, provides a long-term record of daily temperature and precipitation. Continuous records from 1982–2023 were compiled. The mean annual temperature at the station is approximately 0.1 °C (1982–2023 average), ranging from mean monthly lows of -18.6 °C in January to highs of 16.4 °C in July. Mean annual precipitation is ~953 mm at the station. The WSP 2024 adjusted climate data for the region was used. Using Ouranos regional climate normal, the station data were adjusted for the Troilus site: e.g. winter precipitation 16% lower at site, summer 13% higher, reflecting local topography and latitude (WSP 2024). After adjustment, the site's mean annual precipitation is ~960 mm (i.e. ~0.7% higher than the raw station value), and mean annual temperature about -1.1 °C. These adjusted climate inputs (daily temperature and precipitation) were used to drive the baseline hydrologic simulations.
- **Field Hydrology (Wachiih 2024):** Wachiih Resources (2024) provided site-specific hydrological monitoring data from a field campaign in 2023. This included continuous water level measurements (May–October 2023) at key locations: Lac A, Lac Amont, and three local streams, along with three discrete flow measurements.
- **Rating Curves and Stage-Discharge:** The Wachiih (2019, 2024) field programs provided limited flow measurements with which to construct rating curves (water level vs. flow) for the streams. Despite these efforts, the rating curves remain a source of uncertainty due to the low number of points and the short monitoring period. Especially at higher flows, extrapolation was required.
- **Groundwater Recharge:** Recharge rates from the WSP hydrogeological model (Chapter 10) guided baseflow parameterization, ensuring consistency between surface and subsurface water budgets.
- **Land Cover and Curve Numbers:** Land use/land cover (LULC) information was obtained from site mapping WSP terrain analysis 2021 and used to assign SCS Curve Numbers in the model. Curve Number assignments were based on WSP (2024) Appendix D classifications. Table 1-1 summarizes the CN values applied to each major land cover type in the model, reflecting pre-mine and mine development conditions. These CN values were applied to sub-basins according to the expected future land use (e.g. areas to be cleared or built-up were given higher CNs The CN table illustrates the contrast between undisturbed forest (CN ~60) versus mine surfaces (CN 86–91), which is critical in predicting increased runoff from mine development.

Table 1-1: Curve Numbers for predominant land cover types in the hydrology model (source: WSP 2024 data).

Land Cover / Terrain Type	SCS Curve Number
Overburden dumps, built areas	91
Cleared mine site (disturbed soils)	86
Waste rock dumps	72
Natural wooded areas	60
Wetlands (organic soils)	71

- **Mining Operation:** The WSP GoldSim output (WSP, 2024) was used to represent mining operations in the HEC-HMS model. This output includes projected water use for the ore processing plant, tailings storage facility (TSF), and water treatment plant (WTP). The water is routed to sumps and sediment ponds, which are explicitly represented in the HEC-HMS model, along with the associated pumping systems. These components were implemented based on the designs provided by WSP in Appendices E and G of the Site-Wide Water Management Plan. Figures 1-1 and 1-2 illustrate the schematic of the modeled processes as well as design parameters for sediment ponds and sumps.

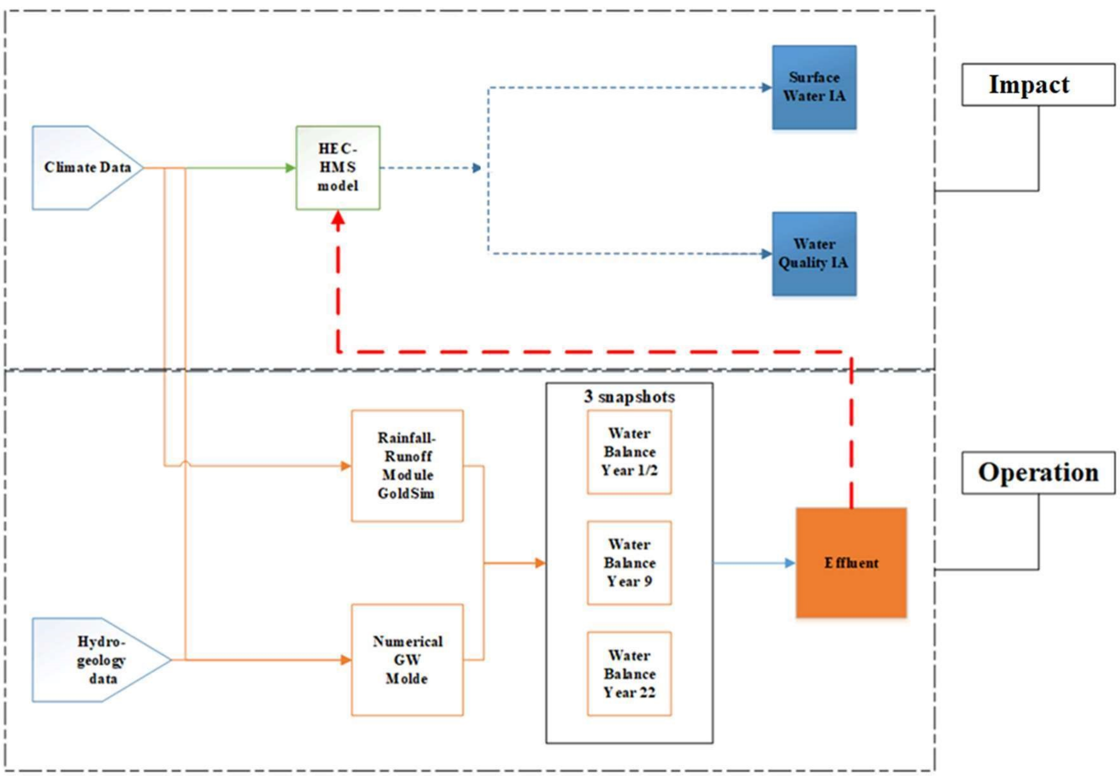

Figure1-1: Schematic presentation of hydrology modelling and the input data

Parameter	Unit	SP01	SP02	SP03	SP04
Total Drainage Area (including Ditches; not including pumping)	km^2	0.98	3.02	1.55	2.25
Upstream Inflow Sources	-	S01 / S01b pumped flows	S06 pumped flow	S05 pumped flow	S09 Pumped flow
Outlet to	-	DC1	DC1	Lake A Inlet Channel	Lake A Inlet Channel
Pump Capacity	m^3/s	0.4	1.0	1.0	1.0
Total Required Footprint	ha	4.3	14.9 (87 Pit Phase 0)	5.6	6.6
Shape	-	Rectangular	Irregular	Rectangular	Rectangular
Available Live Storage Volume	m^3	74,500	516,000	83,000	145,000
Required Live Storage Volume	m^3	63,000	150,000	80,000	125,000
Dead Storage Volume	m^3	8,800	127,700	11,600	18,400
Total Containment Volume	m^3	79,000	757,900	99,600	156,000
Excavation Volume	m^3	192,100	757,900	223,100	420,700
Length at Live Storage	m	187	87 Pit Phase 0 - Pit Shell	325	202
Width at Live Storage	m	120	87 Pit Phase 0 - Pit Shell	98	256
Depth (top of lining)	m	4.0	45	4.0	4.0
Side Slope	xH:1V	3	87 Pit Phase 0 - Pit Shell	3	3
Dead storage allowance	m	0.5	5	0.5	0.5
Freeboard Allowance	m	0	5	0.5	0.5
Minimum Crest Elevation	masl	372.80	330	353.08	354.67
Top of Live storage	masl	372.80	325.00	352.58	354.17
Top of Dead Storage	masl	369.33	300.00	349.58	351.17
Invert Elevation	masl	368.83	285	349.08	350.67
Pond Lining Material	m	1.0 m rock over 0.5 m sandy gravel over NWG	Pit shell	1.0 m rock over 0.5 m sandy gravel over NWG	1.0 m rock over 0.5 m sandy gravel over NWG

Figure 1-2: Sediment Ponds and Sumps Design Parameters (Source WSP 2024)

- **Incorporation of Climate Change:** Future climate projections were integrated into hydrologic analysis in line with guidance from Ouranos and ECCC. The key projected changes (median values for 2021–2050 vs. 1991–2020) include: warmer temperatures by about 1.4 °C annually (with winter warming up to ~1.9 °C) and increased total precipitation by ~6% annually (with a stronger increase in winter +11%, and smaller in summer +4%). These trends – a warmer, wetter climate especially in winter – are consistently indicated across many climate models, although individual projections vary considerably. Table 1-2 from Ouranos (2024) compiles these seasonal changes for SSP2-4.5 Scenario moderate emission. For incorporation into HEC-HMS, the seasonal coefficients were applied to the historical climate data to obtain climate projections. Figure 1-3 shows the mean annual cycle of projected precipitation and temperature.

Table 1-2: Changes for the Period 2021–2050 Relative to 1991–2020 (Ouranos 2024)

Season	Avg Temp Change (°C)			Precipitation Change (mm)		
	10%	50%	90%	10%	50%	90%
Dec. to Feb	1.5	1.9	2.8	10%	11%	15%
Mar. to May	0.6	1.2	1.8	0%	7%	13%
Jun. to Aug	0.7	1.2	1.7	-1%	4%	4%

Sep. to Nov	1.1	1.2	1.6	4%	5%	9%
Annual	1.1	1.4	1.8	4%	6%	8%

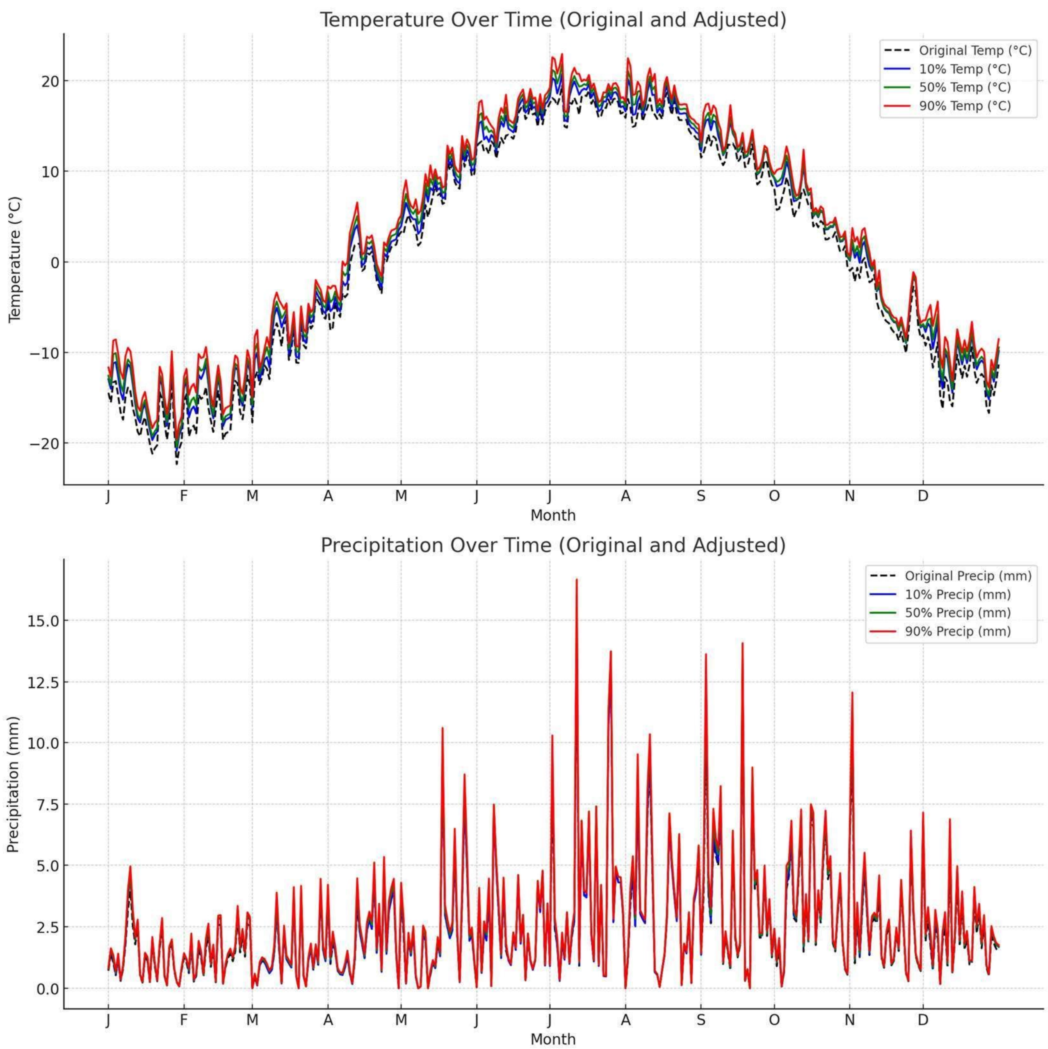

Figure 1-3: Mean annual cycle projection of temperature and precipitation for 2021-2050

1.5 Model Calibration

Model calibration was performed to ensure the HEC-HMS simulations reproduce observed streamflow behavior as closely as possible, within the limitations of available data. Calibration focused on the period of May–October 2023, where continuous observed flows (from Wachiih 2024) were available for Sond #2a (Figure 1-4), which is located immediately upstream of pit 87 on Bibou Creek. Key calibration steps included adjusting curve numbers, initial abstraction, baseflow recession constants, and lag times to minimize errors between simulated and observed hydrographs.

The process included a manual calibration and sensitivity analyses to detect sensitive parameters followed by an automatic calibration using embedded optimization tools offered by HEC-HMS.

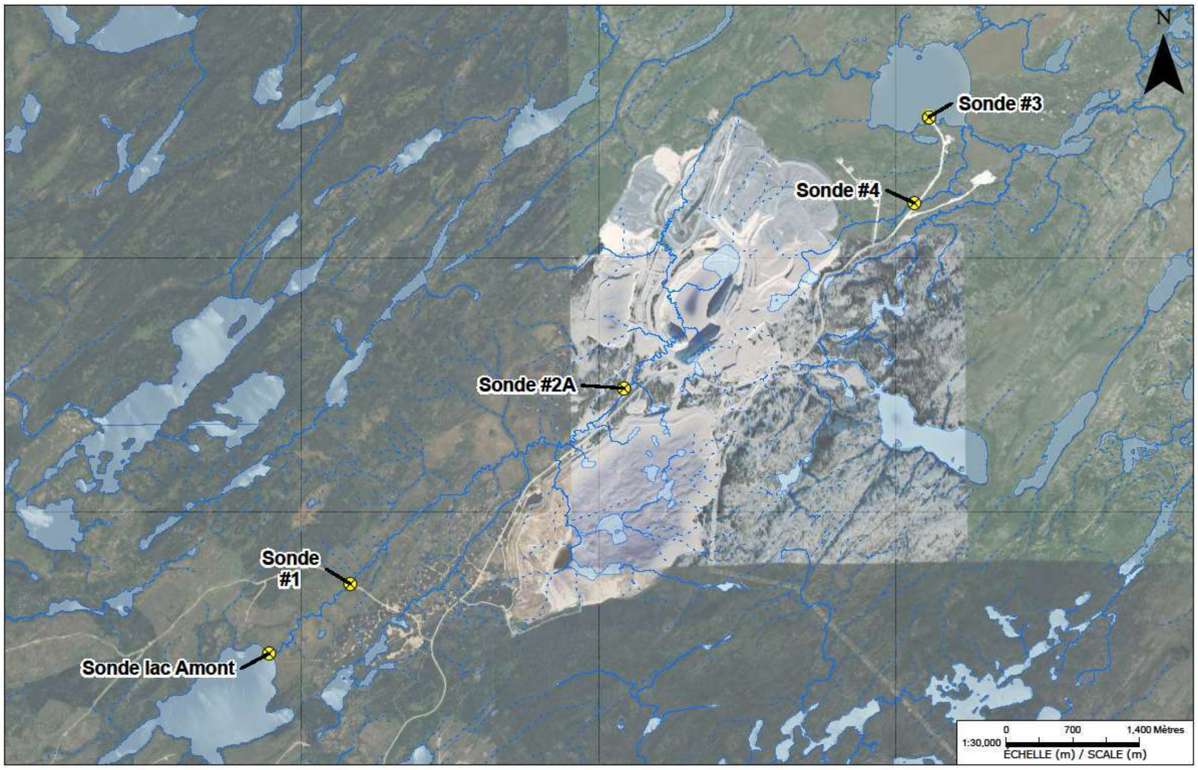

Figure 1-4: Location of measured flow

Calibration involved testing several parameter configurations and comparing model outputs to observed data. Four main calibration approaches were assessed:

- Option 1: Emphasize peak flow matching (higher CN, shorter lag) at the expense of baseflow fit.
- Option 2: Like Option 1 (peak-weighted) with slight adjustments to improve intermediate flows.
- Option 3: Balanced calibration for overall RMSE minimization (moderate CN, inclusion of baseflow contribution).
- Option 4: Alternative balance of parameters to test model sensitivity (slightly higher CN or different recession parameters than Option 3).

Figure 1-5 presents a comparison of the calibration results for these four options, illustrating their relative performance against observed data. As seen, the first two options can better estimate peak flow and timing of the peak, even though they tend to slightly underestimate the maximum peak value. The model overestimates baseflow during summer–fall, yet its simulated hydrograph shape aligns with long-term Broadback River data (Figure 1-6), which exhibits a spring peak in May and a secondary fall peak driven by snowmelt and rainfall.

The observed inaccuracies are likely due to uncertainties in flow measurement and errors that arise when developing rating curves, which tend to accumulate in the lower tail of the flow distribution and affect low-flow estimates. Another contributing factor could be a mismatch between the available climate data and the observed streamflow records.

While the third and fourth modeling options are intended to capture the full variability of the hydrograph, they tend to underestimate peak flows and struggle with accurately timing the peak, especially in the case of snowmelt-driven freshets as observed in option 4. The same type of reasoning provided for options 1 and 2 can explain such behaviors for options 3 and 4. Option 2 was selected for the simulation, as it offered the best overall performance in capturing key flow characteristics, particularly the spring freshet peaks.

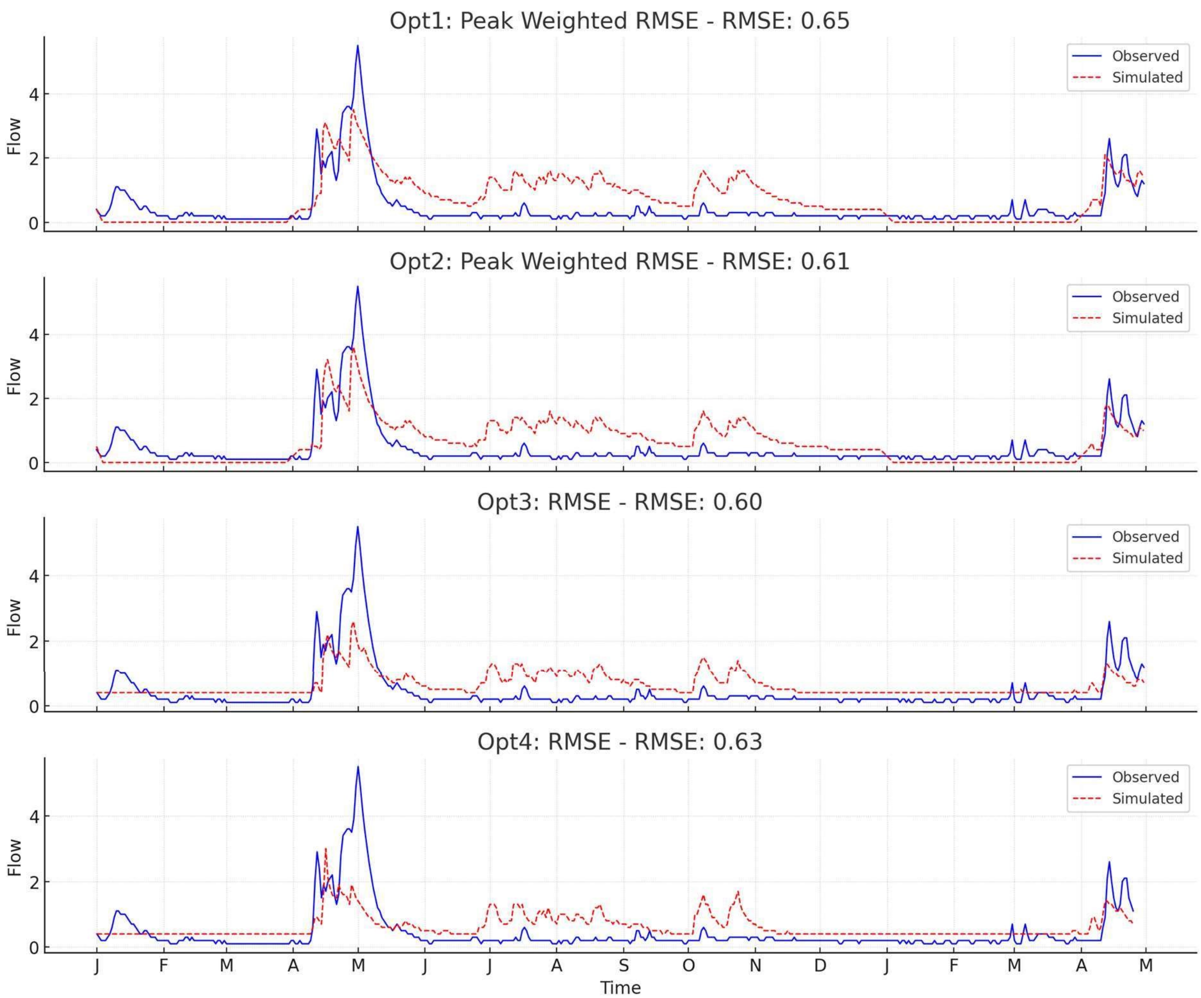

Figure 1-5: Calibration Options for Sonde #2

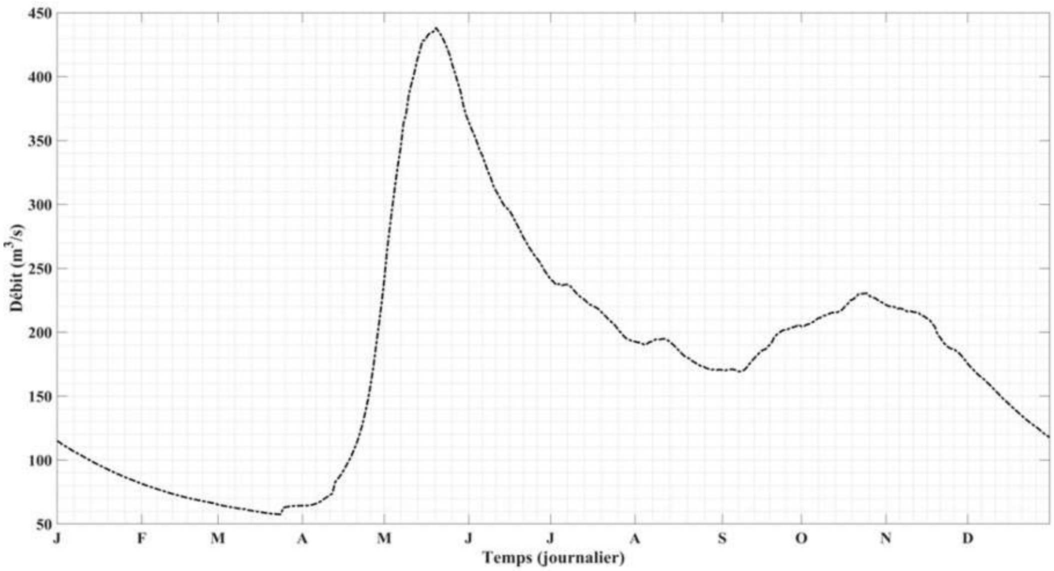

Figure 1-6: Broadback River station mean annual cycle hydrograph (1972 to 2024)

In summary, the calibration process yielded a set of model parameters that provide a reasonable match to observed site hydrology. The calibrated model can simulate both the magnitude and timing of flows for critical periods (spring melt floods and summer rain events) with sufficient accuracy for engineering purposes. Remaining discrepancies (such as slight over-prediction of low flows) are acknowledged and are within the range of measurement uncertainty. These calibrated parameters form the basis for all subsequent hydrological modeling and climate change analyses.

1.6 Results

This section provides the output of HEC-HMS model for multiple scenarios:

- Baseline Scenario: represents the site's existing conditions at present.
- Construction Scenario: the results at the end of construction, before the start of operations.
    - Pit dewatering during construction was not included due to a lack of data.
    - Mining discharge to the environment is assumed to be zero.
    - Only the impact of infrastructure on runoff production is considered.
- Four operation scenarios:
    - Year 1 of operation (Y1), and associated climate change simulation (Y1-CC)
    - Year 21 of operation (Y21). and associated climate change simulation (Y1-CC)

Appendix I provides results for the important hydrological elements. Results for all elements are available upon request (a results summary of all hydrological elements can be found within Appendix II).

1.6.1 Construction Scenario

During the construction phase, a series of activities - such as deforestation, excavation of overburden and vegetation, and the use of explosives - will directly modify the land surface and disrupt natural drainage patterns. Although drainage solutions will be designed and implemented, a change in the hydrological regime is expected. Two monitoring points have been selected to compare construction flow with baseline conditions (Figure 1-7, please refer to Figure 2-1 and 2-2 for more details about the location of different hydrological components of the project):

- PS6 (The junction of the Diversion Channel (DC) /Bibou Creek (CE2) at Lake A (PE43)): This point is monitored to assess the influence of any significant changes in the hydrological regime, as it is the main outlet for the western part of the watersheds draining into Lake A (PE43).
- PS9 (Lake A outlet (PE43)): this point represents the role of Lake A (PE43) in the potential restoration of flows to baseline conditions. It enables us to assess the extent to which Lake A (PE43) mitigates changes to the hydrological regime.

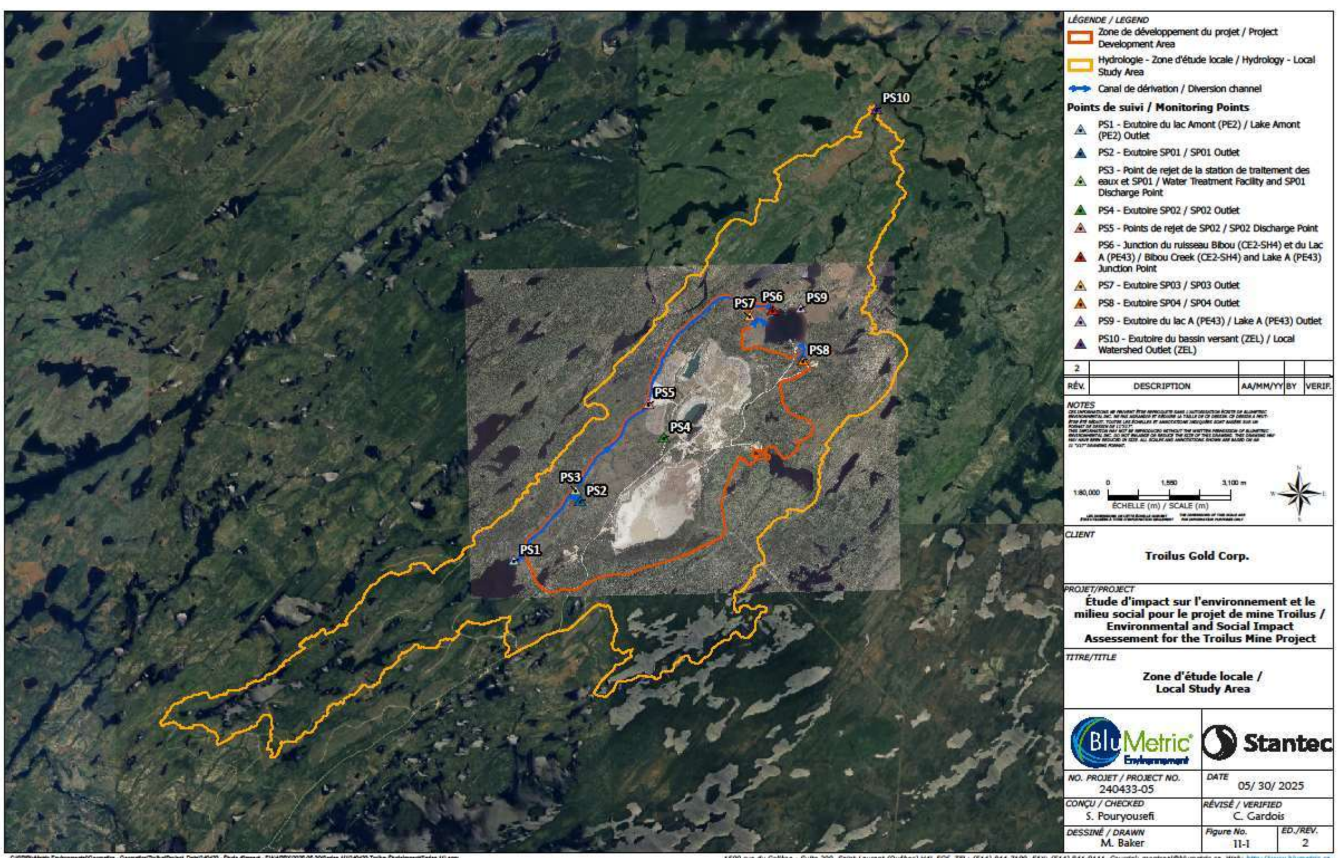

Figure 1-7: Follow up points for scenario comparison

Figure 1-8 compares the mean annual cycle flow at the end of the construction period with that of the reference period for the first selected point.

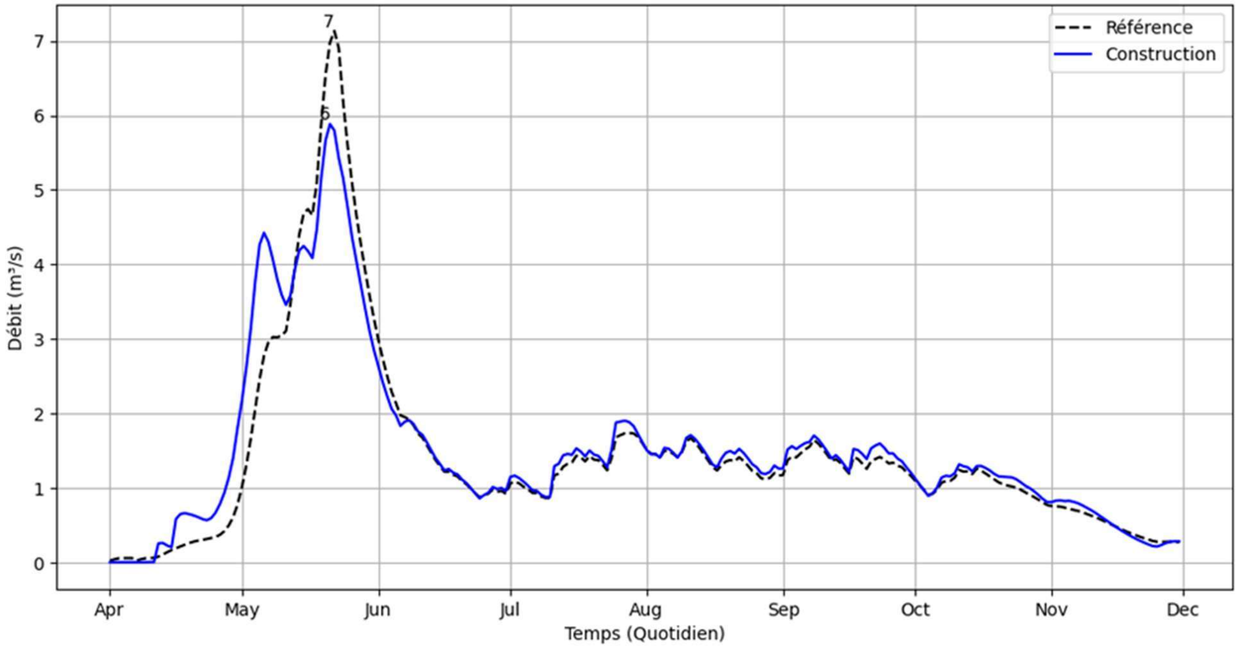

Figure 1-8: Mean annual cycle of simulated flow at the confluence of Bibou Creek (CE2-SH46) with Lake A (PE43)

Key Observations

- Peak flow reduction: the peak flow of the scenario representative of the construction phase will be reduced by 14% compared with reference conditions, i.e. 7 m3/s for reference conditions compared with 6 m3/s during the construction phase. These results suggest that the mitigation measures and water management infrastructure implemented during the construction phase will temper the high flows.
- Summer-fall flows: Overall, daily flows in both scenarios are similar beyond July. However, daily flows during the construction phase will be slightly higher towards the end of summer and into fall.

Activities planned during the construction phase of the project will result in a reduction in peak flows, as well as an increase in base flows. This suggests that the mitigation measures that will be put in place will contribute to the attenuation of flood peaks and help maintain flows during drier periods. Figure 1-9 compares the mean annual cycle flow at the end of the construction period with that of the reference period for the second selected point.

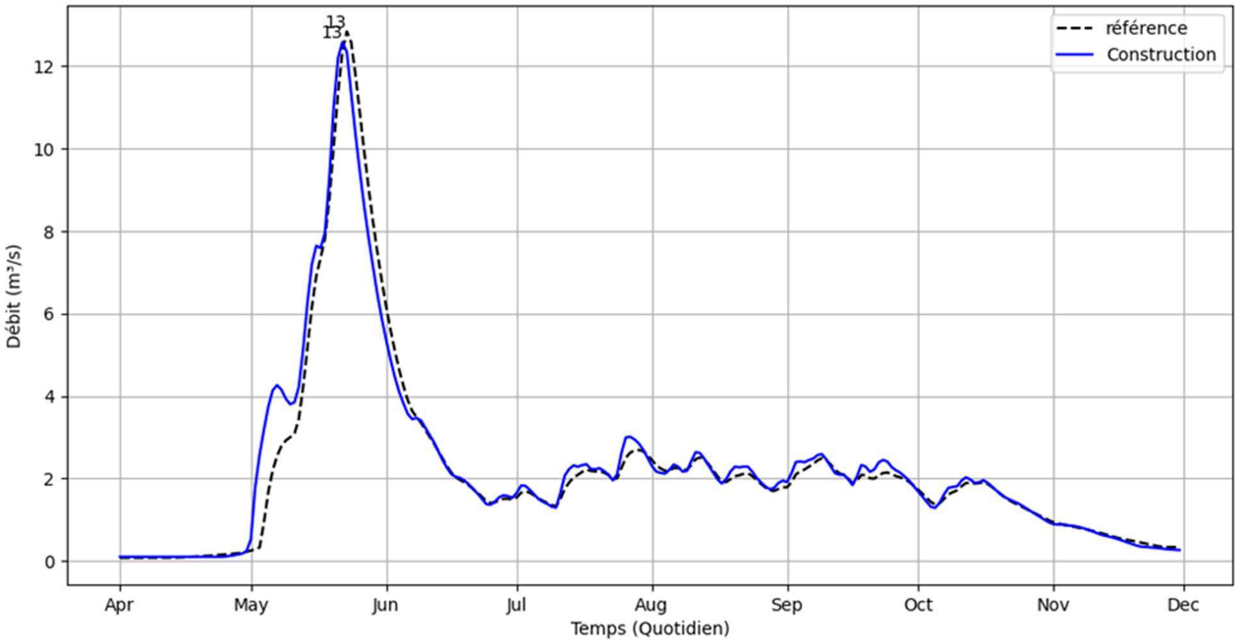

Figure 1-9: Mean annual cycle of flow at Lake A outlet (PE43)

Key observations

- Reduction in peak flow: the peak flow for the scenario representative of the construction phase will be reduced by 1.5% compared with reference conditions. That is, 13.1 m^3/s for reference conditions, compared with 12.9 m^3/s estimated during the construction phase.
- Summer-fall flow: a similar trend to Figure 1.8 is observed in the base flows of both scenarios. Slightly higher flows are anticipated during the construction phase, due to the controlled discharge rate.

During the construction phase, the simulated flood discharge at the outlet of Lake A (PE43) will be slightly lower than that estimated for the reference condition. More specifically, the timing of peak flows appears to be slightly earlier than that of baseline scenario, while the base flow remains unchanged. This observation suggests that the changes made to the infrastructure during this phase will slightly reduce flood peaks, without significantly altering the behavior of the hydrological regime.

1.6.2 Operation Scenario

Mining operation consists of multiple activities include Etraction of ore from the pits, ore processing, mine water management etc. Four points in the watershed were selected for scenario comparisons, which are the outlet of the upstream lake on Bibou Creek/ DC (PS1), the junction of Bibou Creek/ DC with Lake A (PS6), the outlet of Lake A (PS9), and the downstream of the local study area (LSA, PS10).

Figure 1-10 shows the mean annual flow cycle estimated at the junction of Bibou Creek/ DC to Lake A (PE43).

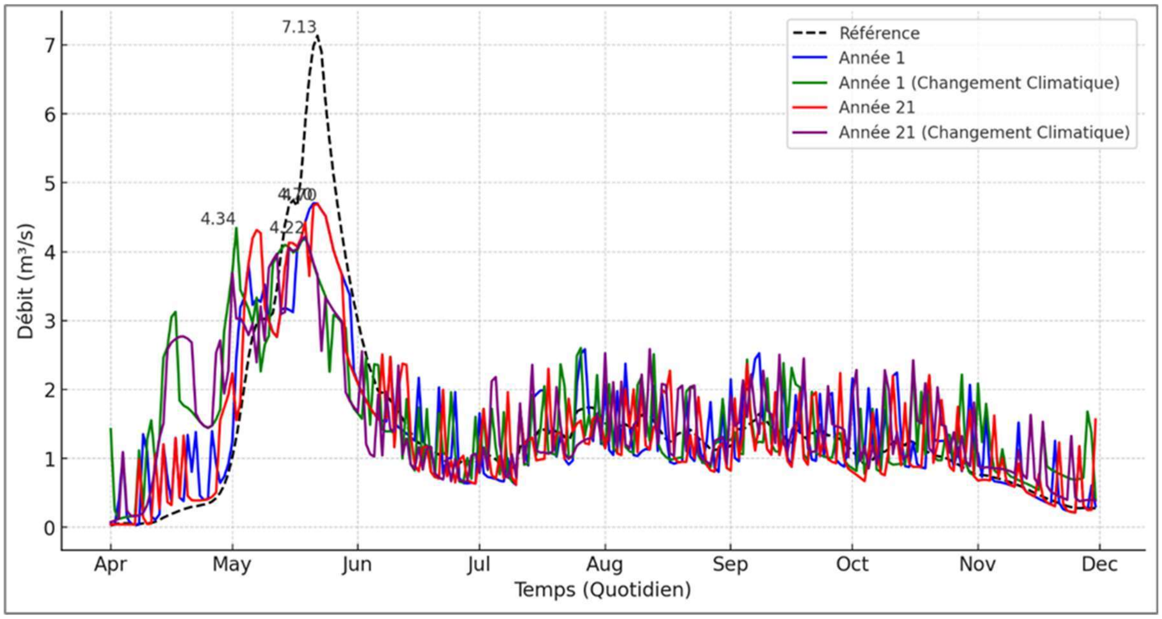

Figure 1-10: Mean annual flow cycle at the junction of Bibou Creek (CE2-SH46) and Lake A (PE43)

- A high degree of variability is simulated between years 1 and 21 of the operation phase and baseline conditions. This variability is mainly due to flow regulation. More specifically, water will be channeled through sedimentation basins, which will modulate flow by attenuating floods and increasing the variability of flood flows. These sedimentation basins will act as a buffer, retaining water during peak precipitation events, resulting in a significant reduction in anticipated peak flows during the construction phase (4.22-4.70 m3/s) compared to the peak flow estimated at 7.13 m3/s for the reference scenario.

- The results of the climate change scenario simulations suggest a noticeable shift in spring flood peak amplitudes compared with historical simulations. Spring floods will occur earlier in the season and will be characterized by lower intensity. This is due to an earlier snowmelt period and lower snow accumulation, contributing to a lower water input to the system during the peak runoff period.
- Like spring freshet period, the operation scenarios show a high variability for summer-fall flow across the scenarios.

For more details about the hydrographs behaviors, a quantile-quantile plot comparing reference (baseline) condition with each scenario have been shown in Figures 1-11 and 1-12:

- During the spring period, all scenarios suggest that flows in the lower end of distribution (< 3 m^3/s) will be magnified, particularly considering climate change scenarios. For flows at the higher end of distribution (> 3 m^3/s), a significant attenuation due to mining activities and water management planning is expected.
- During summer-fall period, the lower end of distribution (<1.2 m^3/s) of scenarios matches with that of reference, for year 1 and 21 scenarios while rise of flow is expected for higher flows (>1.2 m^3/s). This trend inverses for large summer-fall flows derived by intense rainfall (>2.3 m^3/s), which could be attributed to flood attenuation by sediment ponds and sumps.

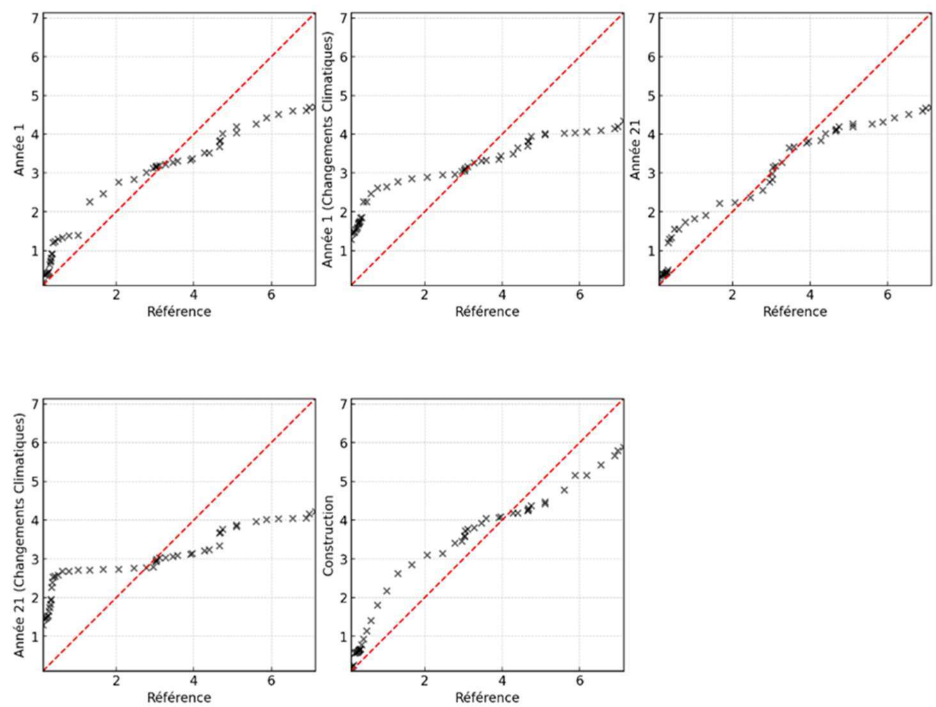

Figure 1-11 : Quantile-Quantile Diagram at PS6 (Spring)

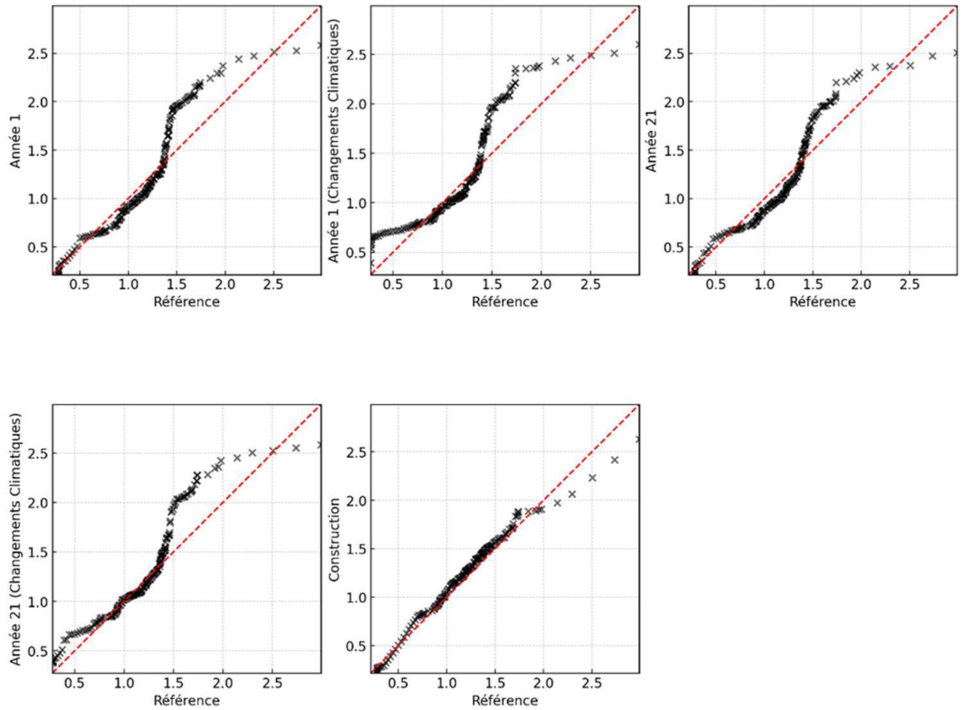

Figure 1-12: Quantile-Quantile Diagram at PS6 (Summer-fall)

Figure 1.13 shows the hydrographs of the mean annual cycle at the outlet of Lake A (PE43) generated for the four scenarios. These hydrographs show low simulate peak flow variability and hydrograph profiles in the operational phase, compared to reference conditions.

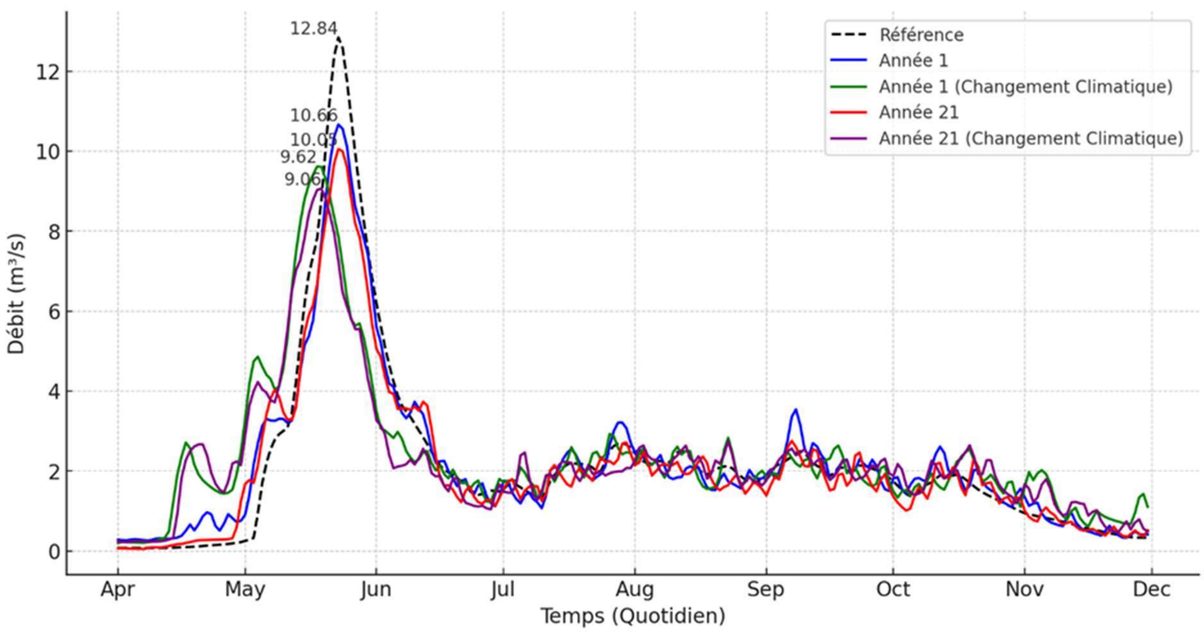

Figure 1-13: Hydrographs of the mean annual cycle of flow at the outlet of Lake A (PE43)

Key observations:

- Lake A (PE43) mitigates the influence of sedimentation basins on the hydrological regime, as a more natural behavior is observed compared to Figure 1.10.
- Peak flows in the operation phase scenarios (Year 1 and Year 21) will remain lower than those observed under baseline conditions, indicating that upstream flow regulation will have an impact on overall flow.
- Climate change scenarios show earlier snowmelt and lower peak flow estimates.

Figures 1-14 and 1-15 compare the distribution of estimated flows for all scenarios with those for the reference state.

- Like PS6, in spring, a higher low flow (< $3m^3/s$) and lower high flow (> $3m^3/s$) is simulated for operation scenarios compared to baseline, which is attributed to flow regulation by water management infrastructure.
- The distribution of estimated summer-fall flows is like that observed in the reference condition for the lower quantiles (except climate change scenarios). Increased variability (increase and then decline from the baseline) is observed at the upper quantiles across all seasons, corresponding to the peak flows of the scenarios.
- The climate change scenarios show a more pronounced deviation at the lower and upper quantiles compared to the reference state. This is mostly due to the climate data as higher precipitation increases low flow while higher temperatures cause lower snow accumulation and decline of spring freshet.

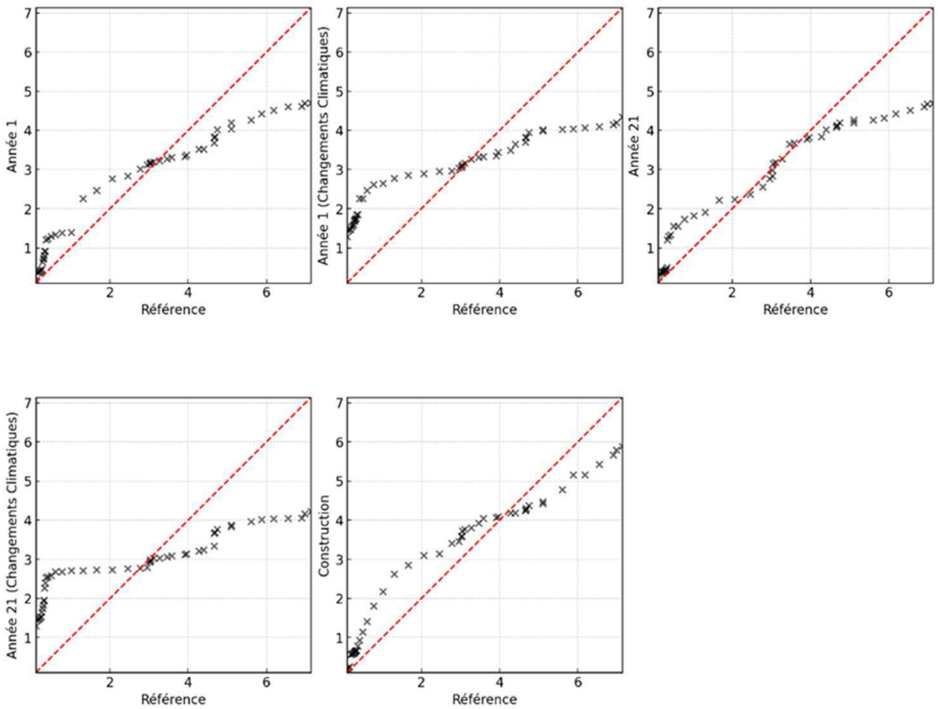

Figure 1-14: Quantile-Quantile Diagram at PS9 (Spring)

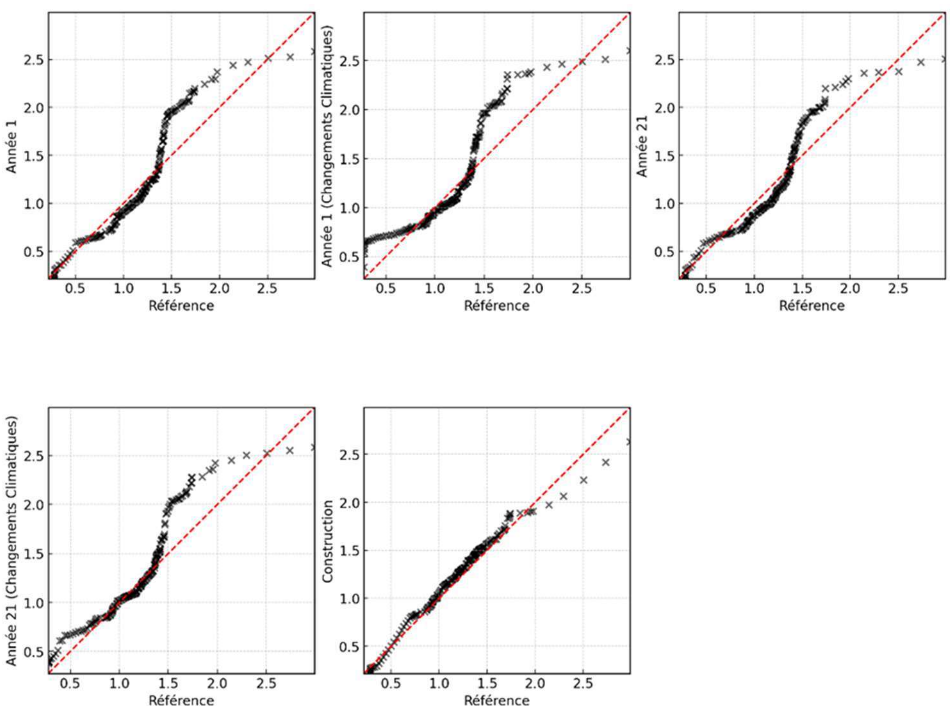

Figure 1-15: Quantile-Quantile Diagram at PS9 (Summer-fall)

Figure 1-17 shows the mean annual hydrograph at the LSA outlet for the four scenarios.

- A pronounced flow peak can be observed at the end of May. This peak reaches 20.10 m^3/s in the scenario representing reference conditions. The scenarios representing Years 1 and 21 of the operation phase show simulated peak flows that are lower than baseline conditions, with a maximum flow of around 18.66 m^3/s for Year 1 and 17.33 m^3/s for Year 21.
- Climate change influences the hydrological regime, with attenuated and earlier peak floods. This is illustrated by a maximum discharge of 16.28 m^3/s for Year 1 and a similar trend for Year 21 (Figure 1.-17).

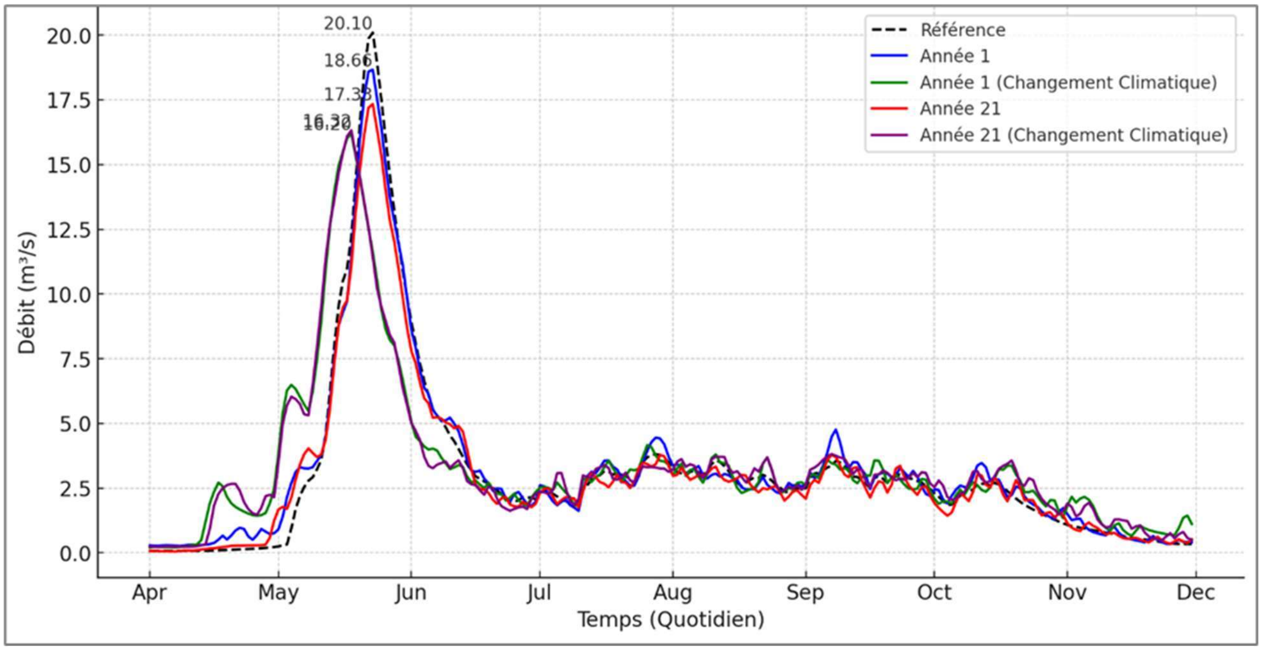

Figure 1-16: Hydrographs of mean annual cycle flow at local study area (LSA)

Figures 1-17 and 1-18 present the quantile–quantile plot at the LSA outlet. Here, the reference scenario's flow quantiles align more closely with those of the other scenarios than at the locations shown in Figures 1-11, 1-12, 1-14 and 1-15. This closer alignment indicates that, by the time flow reaches the LSA outlet, the influence of water-management infrastructures has diminished and the hydrograph has effectively returned to its natural regime.

- During spring, the lower-tail flows in the operation scenarios exceed those of the reference period, while their upper-tail quantiles lie below the reference. In every case, the climate-change scenarios amplify these deviations.
- During summer–fall, the operation scenarios closely match the reference period, aside from minor mid-quantile deviations in Years 1 and 21. At the highest quantiles, operation years show slightly lower flows, indicating reduced runoff during intense precipitation events.

Climate-change scenarios—reflecting regional shifts rather than project effects—elevate low flows and substantially suppress high flows in this season.

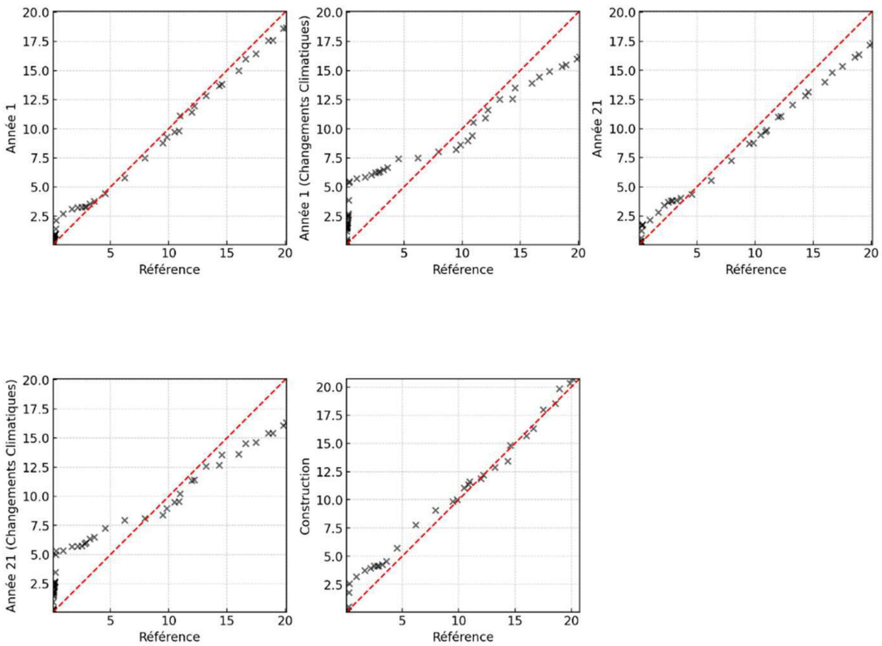

Figure 1-17 : Quantile-Quantile Diagram at PS10 (Spring)

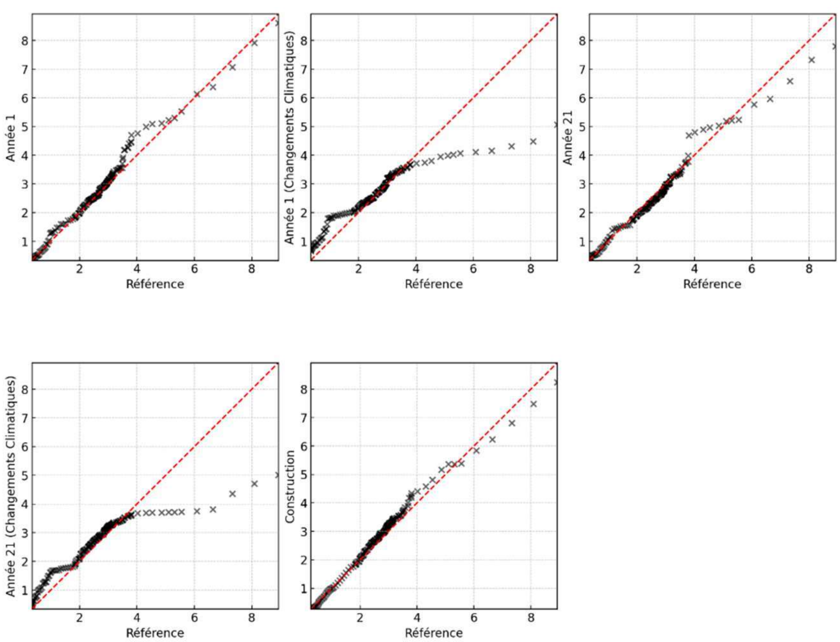

Figure 1-18: Quantile-Quantile Diagram at PS10 (Summer-fall)

Figure 1-19 shows the percentage change in estimated peak flow at the various monitoring points in the LSA, compared with the reference condition.

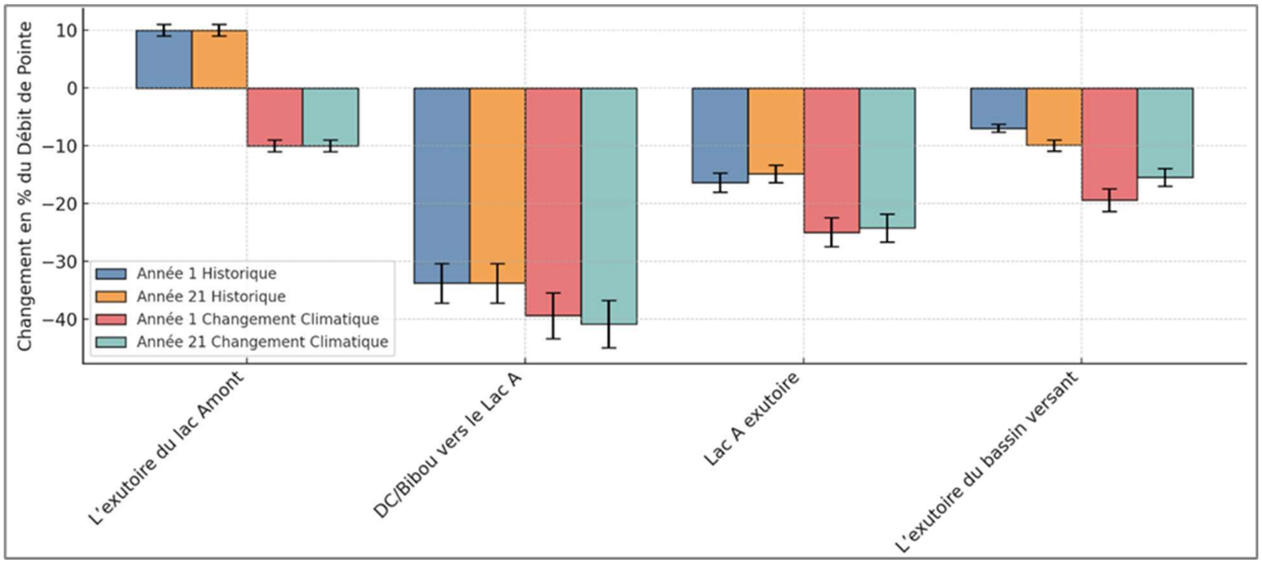

Figure 1-19: Variations (%) in peak flows for each of the four scenarios

At the monitoring point upstream of the PDA (PS1):

- Peak flows increase slightly (≈10%) in all reference scenarios, suggesting a limited change in flows, probably due to variations in groundwater recharge.
- For scenarios associated with climate change, a slight decrease is projected, probably due to a lower snow accumulation and spring freshet.

At the junction of Bibou Creek with Lake A (PS6):

- Anticipated peak flows are greatly reduced (≈-35%), indicating significant flow regulation due to the sedimentation basins, which will act as a buffer by attenuating floods.
- For climate change scenarios, the reduction in projected peak flow is greater than for baseline scenarios.

At Lake A outlet (PS9)

- This trend continues at the outlet of Lake A (PE43), where reductions in simulated peak flow remain significant (-10% to -15%), although less marked than at Bibou Creek (CE2).
- For the climate change scenarios, the reduction in projected peak flow is greater than for the baseline scenarios, as we have seen previously

At the watershed outlet (PS10):

- Decreases in simulated peak flows at Lake A outlet (PE43) persist (-5% to -10%), although they are less pronounced than at upstream monitoring points.
- Like the other selected points, climate change further decreases the projected peak by an extra 5 to 10% compared to status quo scenarios.

These findings suggest that the project's water management measures may be contributing to lower peak flows, potentially reducing the likelihood of higher discharges and additional inundation during spring freshet.

Figure 1-20 shows the percentage change in total volume estimated at the various monitoring points in the LSA, compared with the reference state of the current environment.

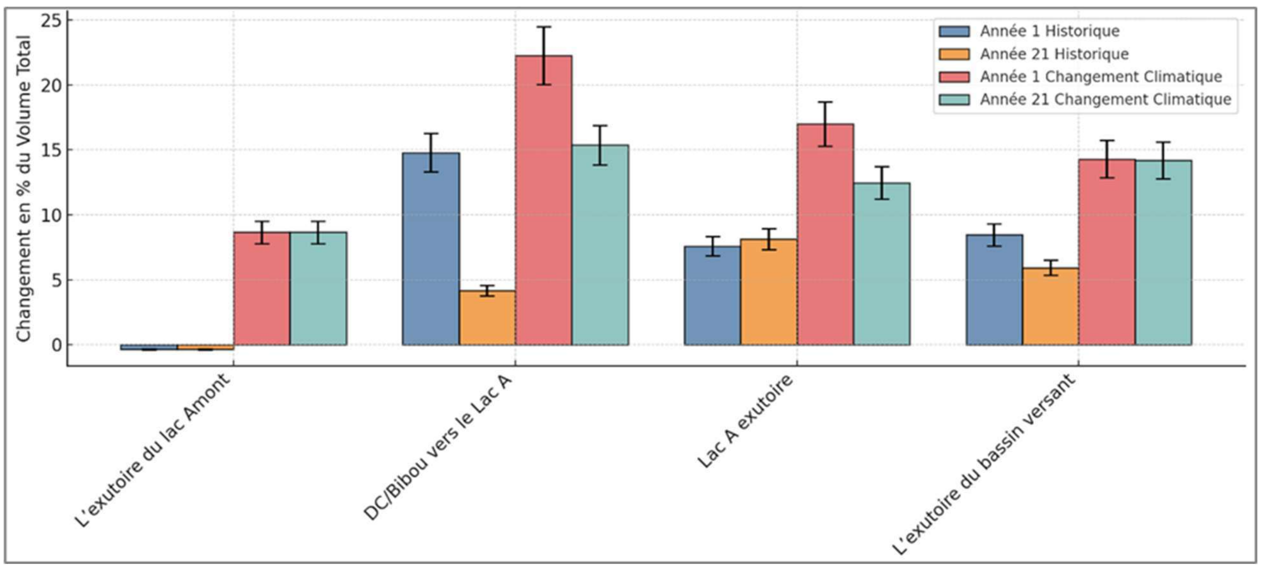

Figure 1-20: Rate of change (%) of total volumes estimated at the various LSA monitoring points compared with the reference state

At the monitoring point upstream of the PDA (PS1):

- Slight variations are expected across all scenarios, indicating that upstream flows will remain unchanged overall.
- An increase of less than 10% is estimated for scenarios associated with climate change. Since the impact of the project at this point is negligible, the variation of around 10% in total volume can be explained exclusively by the climate change signal.

At the junction of Bibou Creek with Lake A (PS6):

- A 15% increase in total volume is estimated for the Year 1 business-as-usual scenarios, due to the impact of activities planned during the operation phase, such as pit dewatering and mine effluent discharge. This estimate remains below 10% for Year 21, indicating negligible variation in the volume anticipated for this scenario.
- The climate change scenario shows around 10% increase in projected volume at this location.

At Lake A outlet (PS9)

- The total anticipated volume for the status quo scenarios will increase by less than 10%.
- The rates of change are more pronounced in the climate change scenarios (an extra 10% increase).

At the watershed outlet (PS10):

- The total estimated volume will increase slightly (~<10%), but to a lesser extent than at the Lake A (PE43) outlet, indicating that although flow regulation affects total volume, its impact will gradually diminish downstream.
- Like the other selected points, climate change further increases the projected total volume by an extra 5 to 10% compared to status quo scenarios.

These results suggest that total volume may rise, and consequently, significant water-availability issues attributable to the project or climate-change impacts are not expected.

Figure 1-21 shows the percentage change in the estimated summer-fall flow at the various monitoring points in the LSA, compared to the current reference state of the environment. Lake Amont is not shown here because no significant change was observed in the summer-fall flow at this point.

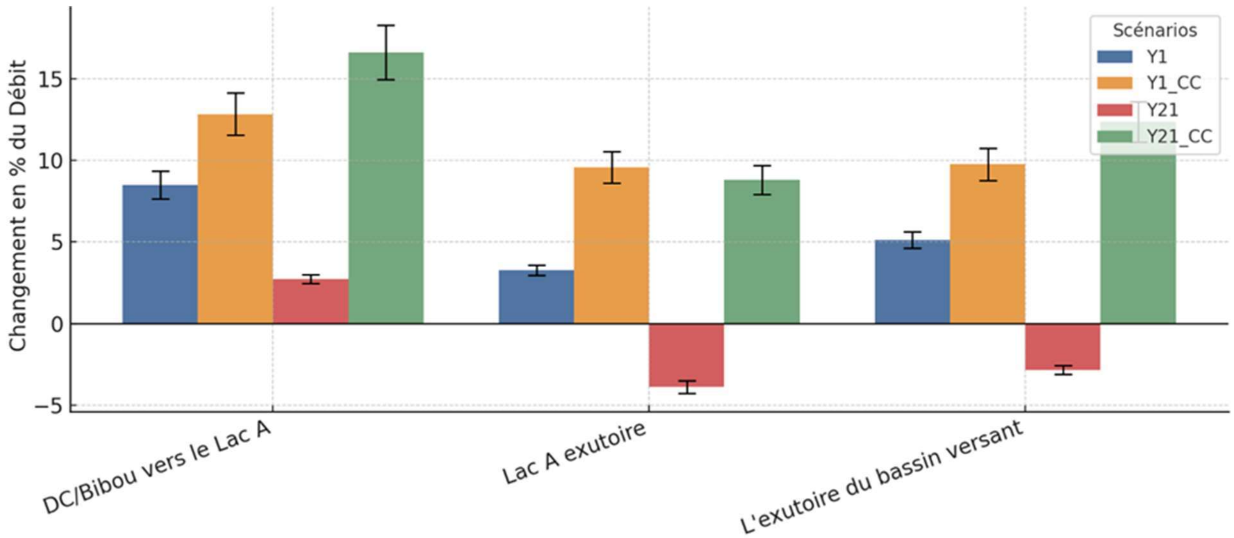

Figure 1-21: Rate of variation (%) of the simulated summer-fall flow at the different monitoring points of the ZEL compared to the reference state

- The simulated rate of change remains below the 10 % threshold across all monitored points evaluated without climate-change impacts, indicating that the project's effect on low‑flow discharge in these scenarios will be negligible.
- However, when accounting for the impacts of climate change, the estimates for the corresponding scenarios show a significant increase in low‑flow discharge (> 10 %) at certain locations and under certain scenarios.
- Unlike the earlier cases for peak flow and total volume, the Year 21 scenario exhibits decrease; nevertheless, because these remain below 10 %, no significant impact on low flows (summer–fall) is expected.

1.7 Discussion

The main changes anticipated by the end of the operating phase are a reduction in peak flows and an increase in summer–fall flows. These impacts stem from the mining operations themselves, the water-treatment systems in place, and alterations to key hydrological parameters.

The projected residual impact on the hydrological regime varies among the different monitoring locations upstream and downstream of the ZDP. At the outlet of Upper Lake (PE2), analysis indicates only minor changes, with negligible variations in estimated flow. A more pronounced change is expected at the junction where the Bibou stream (CE2-SH4) enters Lake A (PE43). At Lake A outlet (PE43) itself, a substantial alteration is anticipated, driven by upstream water retention from both the planned mining activities and the implemented water-management systems. Downstream, at the watershed outlet (ZEL), the change is moderate: peak flows vary slightly, and total volume increases.

Climate change projections further show a significant decrease in the peak flow, an earlier timing of the peak, as well as higher annual volume and summer-fall flow. These changes in general can be attributable to the rise of temperature that causes lower snow accumulation and early melt, as well as rise of liquid precipitation particularly for summer-fall period resulting in higher summer-fall flow and total annual volume. Such changes are in line with the extensive scientific studies carried out (Blöschl 2022, Merz 2022 ,Riboust 2016). Consequently, it is unlikely that the project's hydrologic footprint will be aggravated by these climate-change signals.

These hydrological alterations will continue steadily throughout the operating phase. Moreover, some impacts arising during operation may persist beyond both the operational and mine-closure phases—for example, changes to the watershed's area resulting from construction works. This lingering residual impact is due to modifications of the site's water-retention structures. Consequently, long-term shifts in hydrological parameters affecting infiltration, groundwater levels, and drainage pathways could endure well after site closure.

1.8 Assumptions, Limitations, and Uncertainties

The hydrology model and results are subject to several assumptions and limitations, as well as uncertainties attributed to input data and methods. Key considerations include:

- **Empirical Model Assumptions**: The use of SCS Curve Number and SCS Unit Hydrograph methods implies an assumption that watershed response can be represented by empirical relationships derived elsewhere (mid-continental U.S. conditions). While these methods are standard and were deemed appropriate, they may not capture all site-specific nuances (e.g. nonlinear saturation behavior, complex runoff timing in a lake-chain system). The CN method assumes uniform land surface properties within each sub-basin and an average soil moisture condition. If actual conditions deviate (e.g. localized saturated areas or routing complexities), model accuracy could suffer.
- **Single-Station Climate Data:** The model relies on one primary climate station (Chibougamau Chapais A) for all precipitation and temperature input. This assumes that spatial variability in precipitation across the ~130 km distance is minor after adjustment. Convective summer storms or snow distribution could differ at Troilus. The adjustment factors applied (colder and slightly redistributed precipitation) are based on long-term climate normal and cannot account for single-event differences. This limitation means that some events may be misrepresented – e.g. a local thunderstorm at Troilus might not be captured by the Chapais data, leading the model to under-predict a peak flow, or vice versa.

- **Limited Calibration Data:** The scarcity of observed streamflow data is a significant limitation. This constrains confidence in parameter calibration as multiple different parameter sets could potentially fit the sparse data (equifinality). The chosen calibration (Option 2) provided a reasonable match, but with so few observations, it is possible that the model is not uniquely validated. For instance, no observed extreme flood was captured in 2023 (flows were modest, <6 m^3/s). The model's behavior in a truly extreme event is unverified and rests on extrapolation. The rating curves used to infer flows have inherent uncertainty due to limited measurements. At elevated water levels, the actual flow may vary if the assumptions regarding the cross-section or roughness are inaccurate.
- **Baseflow Representation:** Using an exponential recession for baseflow is a simplistic representation of complex groundwater processes. It assumes a single linear reservoir for groundwater in each basin. Real groundwater flow may have multiple pathways with different time lags. The model may not capture seasonal groundwater dynamics such as delayed late-winter baseflow reductions or rapid recharge events during snowmelt. Nonetheless, by calibrating the recession constantly observed late-season flows, we assume baseflow is reasonably approximate for average conditions. Extreme drought or multi-year trends in groundwater (not modelled) could lead to deviations in actual baseflow that the model would not predict.
- **Snowmelt and Winter Uncertainties:** The temperature-index snow model assumes melt rates proportional to air temperature and does not explicitly simulate mid-winter melt/refreeze cycles or wind redistribution of snow. Unusual events, such as rain-on-snow in mid-winter or rapid temperature swings, might not be well captured. Moreover, the spatial variability of snow and the presence of ice on lakes (which can delay the runoff response) remain simplifications. We assume lakes start to convey outflow only once ice breaks up, but some under-ice flow could occur.
- **Future Climate Projection Uncertainty:** While climate-adjusted scenarios were modeled, they carry significant uncertainty. The use of a single scaling factor and median seasonal shifts approximates complex future changes. Actual future conditions could be wetter or drier than expected. Moreover, the temporal distribution of changes (e.g., more frequent heavy storms vs. steady increases) can impact results differently than a uniform factor. The model's future scenario results should thus be viewed as potential outcomes rather than precise predictions.
- **Data Quality and Resolution:** Some input datasets have limitations. The 1 m LiDAR DEM is high-resolution, but small errors or interpolations in flat wetland areas could slightly misrepresent drainage boundaries. Land cover classification might change over the project lifespan; for example, if more area is cleared than anticipated, the Curve Number (CN) values used underestimate runoff, as the model assumes specific extents for each CN class. The

hydrogeology inputs (e.g., recharge rates) are themselves model-derived, so any errors in those estimates propagate into the baseflow calibration.

1.9 Conclusion

Despite these limitations, the hydrologic model is considered fit for purpose when results are interpreted with appropriate caution. The model's structure, which is a combination of proven empirical methods and physically based routing, provides a reasonable representation of the system. Uncertainties have been managed through conservative assumptions, such as using Chapais 2 data for higher rainfall extremes and incorporating climate change factors. Nonetheless, it is recommended that the model be recalibrated and validated as more data becomes available (e.g., expanded stream gauging during operations or the addition of on-site weather stations) to improve accuracy.

In conclusion, the hydrologic modeling for the Troilus Project provides a comprehensive analysis of both baseline and future runoff conditions, using best-available data and standard methods. The results inform environmental impact assessments. Model limitations and uncertainties have been transparently acknowledged. Overall, the model indicates that the proposed water management system can accommodate the range of hydrological conditions expected at Troilus, with a sufficient margin to address climate variability and change. Future monitoring and model updates will further enhance confidence in these projections, ensuring the project remains resilient and aligned with environmental and engineering best practices.

Respectfully submitted,
BluMetric Environmental Inc.

<original signé par>

Siavash Pouryousefi Markhali, Ph.D.
Hydrogeologist

Reviewed by:

<original signé par>

Michael Melaney, M.Sc. Eng., P.Eng.
Senior Engineer, Team Lead – Civil & Environmental Engineering

<original signé par>

Christian Gardois, M.Sc., P.Eng.
Geological Engineer / Senior Hydrogeologist

References

Blöschl, G. (2022). Three hypotheses on changing river flood hazards. Hydrology and Earth System Sciences, 26(19), 5015-5033.

Corporation minière Inmet. 1996. Programme de surveillance et d'inspection environnementale soumis au ministère de l'Environnement et de la Faune Direction régionale de l'Abitibi-Témiscamingue et du Nord du Québec. Projet Troilus

Merz, B., Basso, S., Fischer, S., Lun, D., Blöschl, G., Merz, R., ... & Schumann, A. (2022). Understanding heavy tails of flood peak distributions. Water Resources Research, 58(6), e2021WR030506.

Ouranos. 2024. Climate Portraits (Overview of Historical Climate and of Climate Change Projection) for the Jamésie–Sud Est Region. Downloaded from portraits.ouranos.ca in April 2024.

Riboust, P., & Brissette, F. (2016). Analysis of lake champlain/richelieu river's historical 2011 flood. *Canadian Water Resources Journal/Revue canadienne des ressources hydriques*, *41*(1-2), 174-185.

Tremblay, D. (1995). Essais de pompage Mine Troïlus Chibougamau. Chibougamau: Les laboratoires S.L.

WSP (WSP Canada Inc; Golder Associates Ltd. was acquired by WSP). 2021 Troilus Gold Project – Terrain Mapping Rev0. 04 May 2021.

WSP 2024, Troilus Project Operational Site-Wide Water Management Plan, May 2024

Wachiih Resources. 2019. État De Référence Du Milieu Récepteur Hydrologie. December 2019.

Wachiih Resources. 2024. Hydrology. Reference Study – Troilus Mining Project. Project No.: 141022002. March 2024.

Appendix I

Results

2 Introduction

The following suite of figures presents the mean annual hydrograph for each subbasin and diversion catchment, plotting three fundamental hydrologic variables: Discharge (instantaneous flow in m^3/s, blue), Cumulative Discharge (running total of daily runoff in hm^3, red), and Snow Water Equivalent (snowpack storage in mm, green). For the seven primary baseline subbasins (refer to Figure 2-1 for their location and Section 2.2 for the results) that feed Bibou Creek, these plots reveal how watershed area and elevation influence the timing and magnitude of meltwater pulses. In the diversion catchments (SB_DC1–SB_DC5, Figure 2-1, and Section 2.3), each plot overlays five operational and climate scenarios—Year 0 (end of construction), Year 1 (first year of operation), Year 1_CC (first year with projected climate-change conditions), Year 21 (two decades of operation), and Year 21_CC (twenty-one years plus climate change) to show both immediate and long-term deviations from the baseline (Section 2).

Across all hydrographs, Discharge captures the spring melt peak and subsequent baseflow recession through summer and autumn; Cumulative Discharge quantifies the total seasonal water yield (critical for reservoir sizing and downstream water budgets); and Snow Water Equivalent indicates the seasonal "bank" of water stored as snow and the onset of melt. The multi scenario comparisons demonstrate that operational modifications alone (Year 1 vs. Year 0; Year 21 vs. Year 0) have relatively minor impacts on hydrograph shape and water yield, whereas the climate-corrected scenarios (indicated by CC) consistently show reduced snowpack accumulation, an advancement of melt onset by several days.

Section 2-4 demonstrates the mean annual cycle outflow from the sediment ponds (SP01 to SP04) for different scenarios (Figures 2-14 to 2-17). This is followed by Section 2-5 that shows the water level and storage variability the Lac A (Figures 2-18 to 2-23). Across all six scenarios, Lake A's elevation (blue) and corresponding storage (red) follow the same fundamental seasonal cycle: a gradual drawdown through winter, a rapid rise to a sharp spring peak in late May, a sustained summer plateau, and a slow autumn recession back toward low winter levels. The spring peak reflects snowmelt inflows and reservoir impoundment, while the summer plateau indicates operations holding the lake near its target stage for water supply or process requirements. The annual storage curve mirrors elevation but in volumetric terms ($\times 10^3$ m^3), quantifying the actual water volume change behind the dam. Comparing operational scenarios (Y0, Y1, Y1_CC, Y21, Y21_CC) to the Baseline reveals that the shape and timing of the spring freshet remain nearly identical, but the fine-scale variability grows under the active operating regimes (Years 1 and 21). Those high-frequency oscillations superimposed on the summer and autumn drawdowns are the signature of sediment-pond pumps cycling on and off, temporarily raising or dropping lake stage by a few decimeters each time.

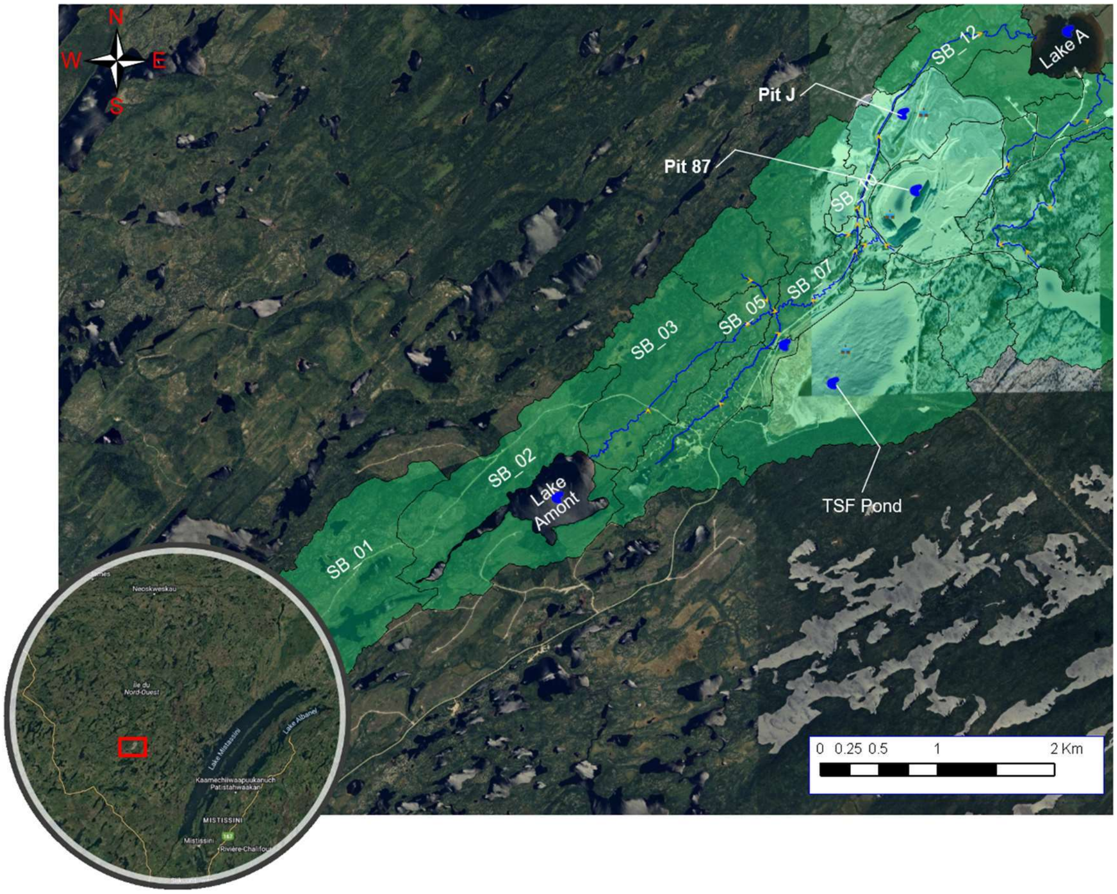

Figure 2-1: Position of selected subbasins and other hydrological elements (Baseline)

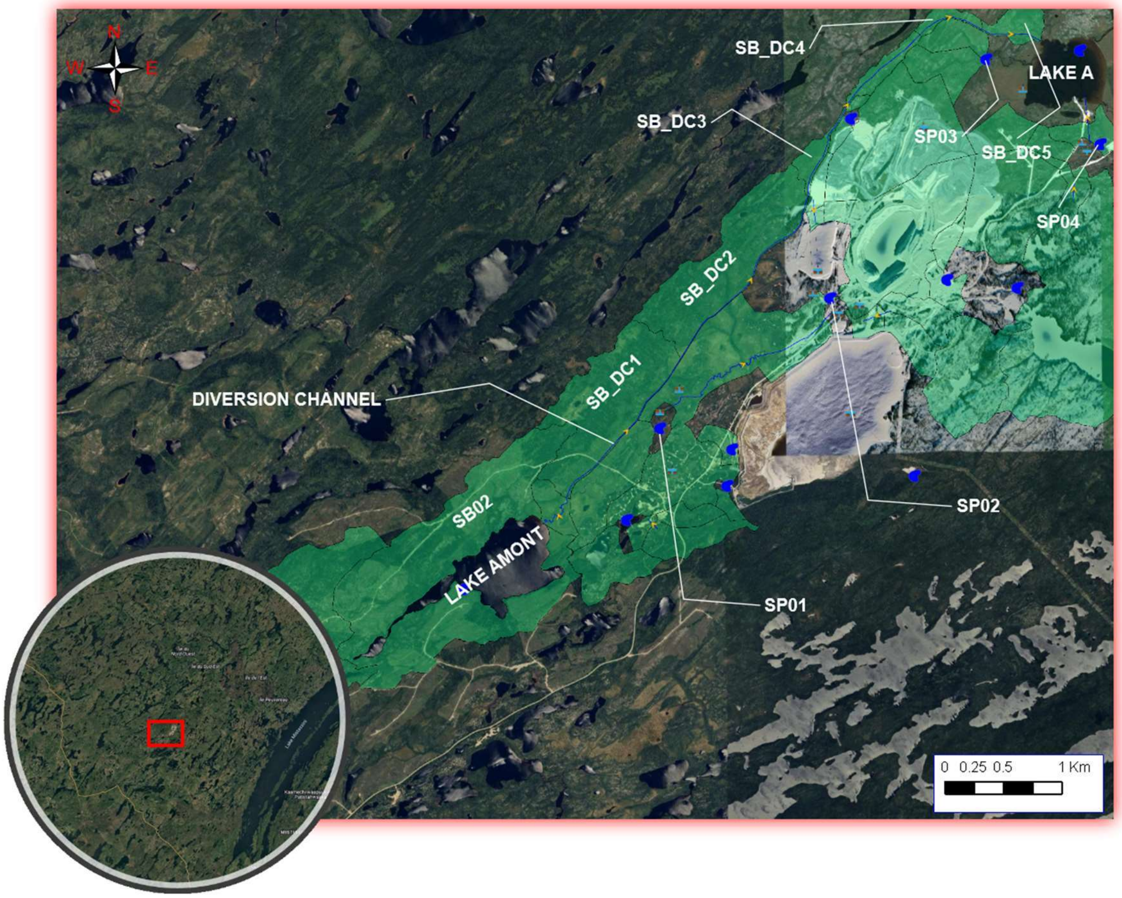

Figure 2-2: Position of selected subbasins and other hydrological elements (operation phase)

2.1 Baseline Hydrographs

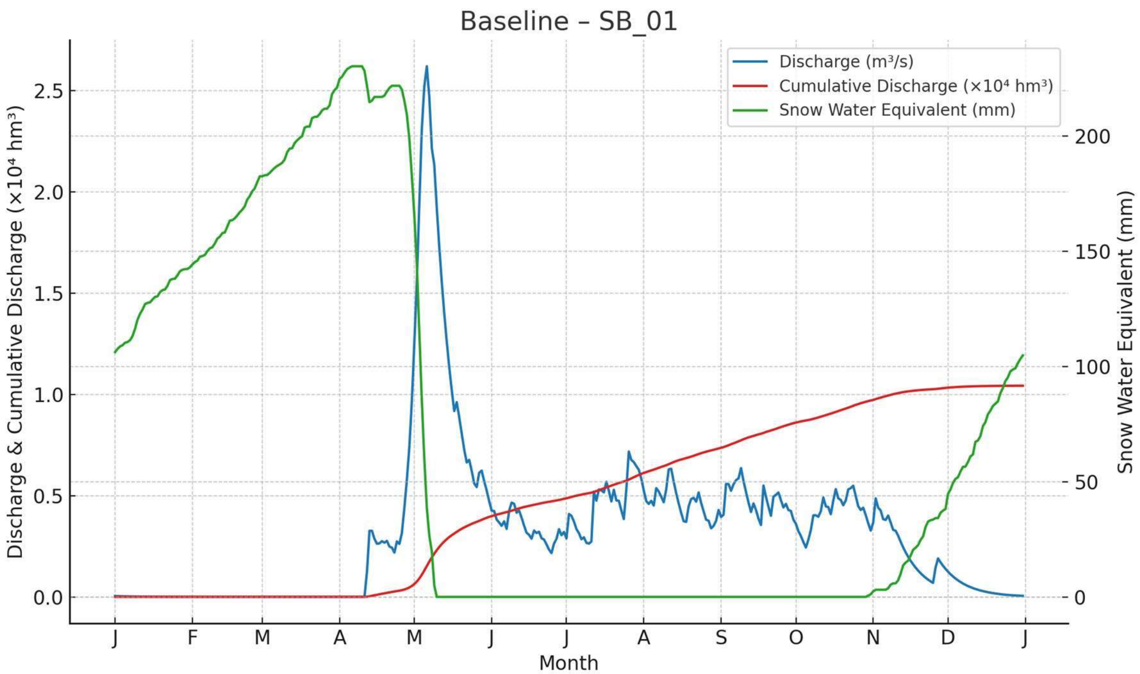

Figure 2-3: Baseline Hydrographs (SB_01)

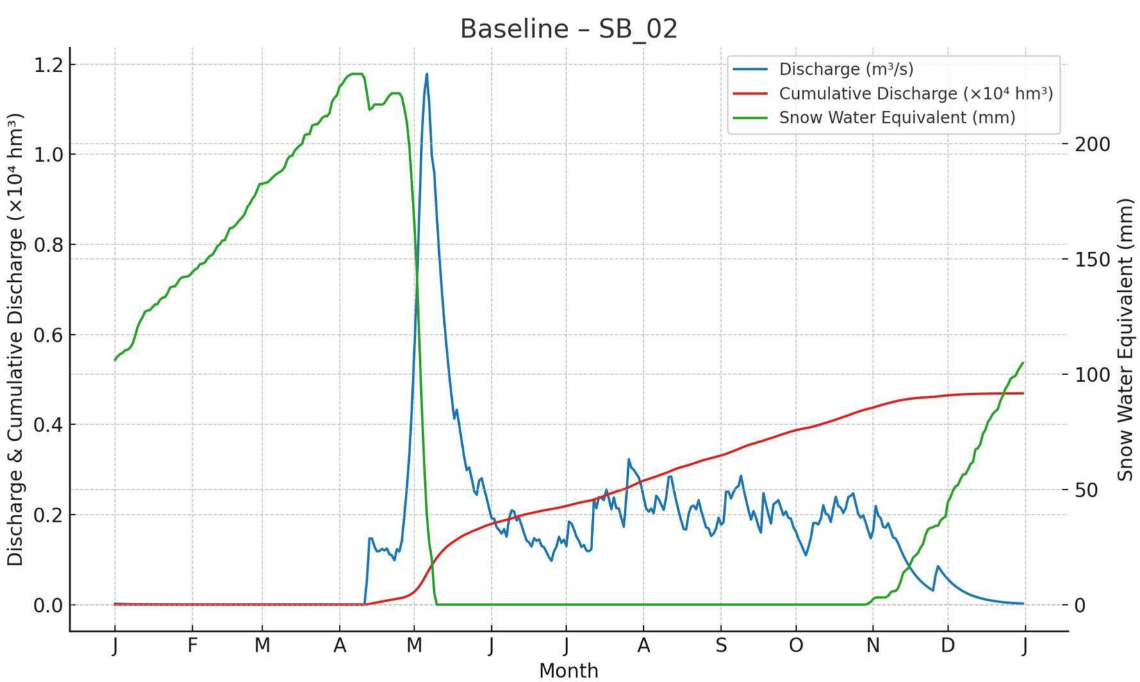

Figure 2-4: Baseline Hydrographs (SB_02)

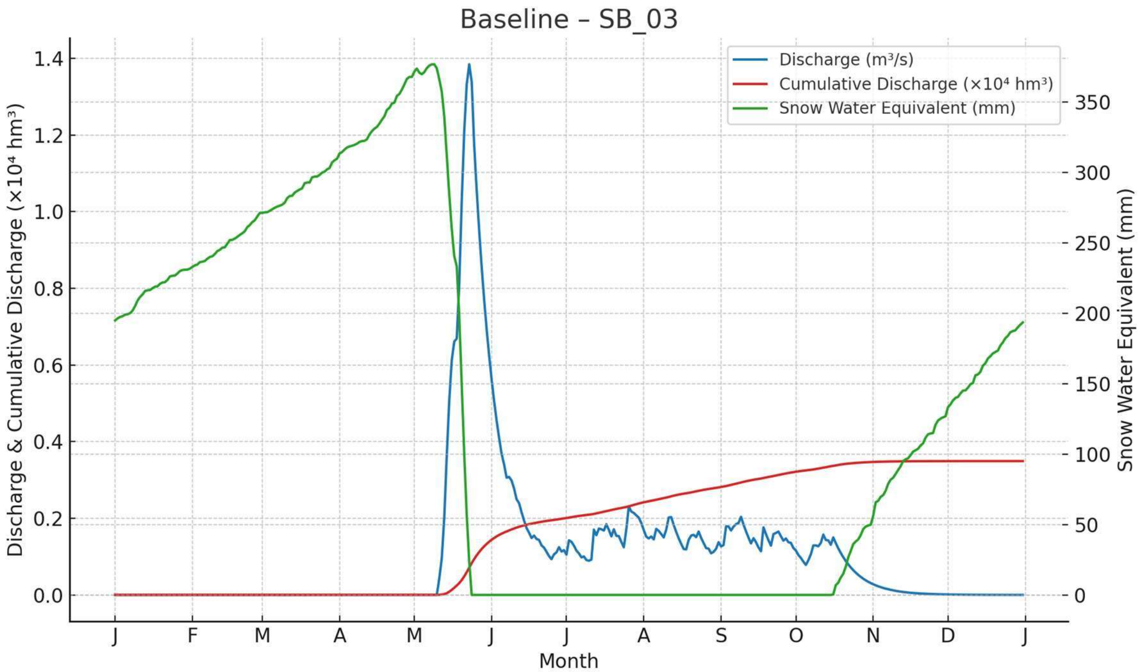

Figure 2-5: Baseline Hydrographs (SB_03)

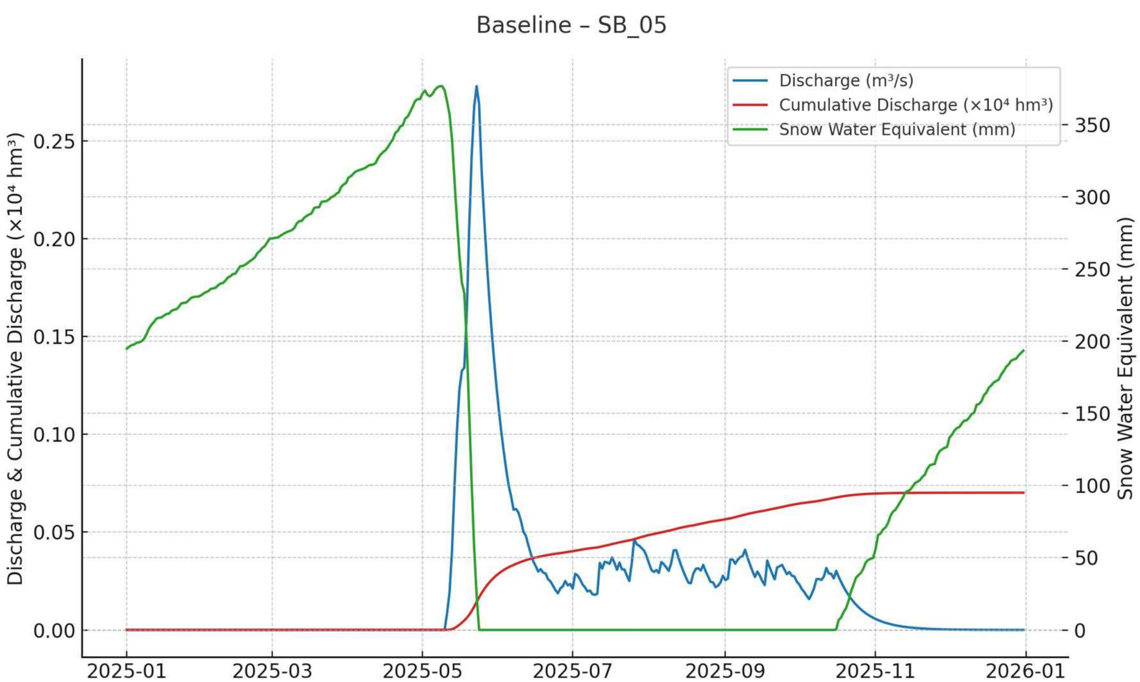

Figure 2-6: Baseline Hydrographs (SB_05)

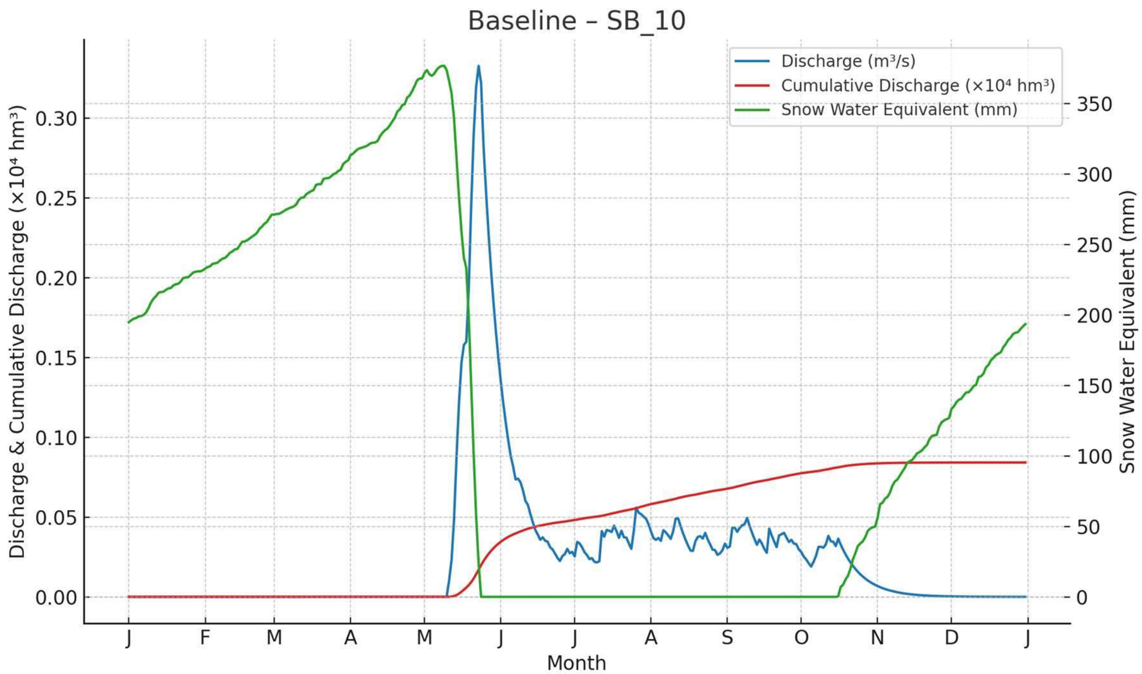

Figure 2-7: Baseline Hydrographs (SB_10)

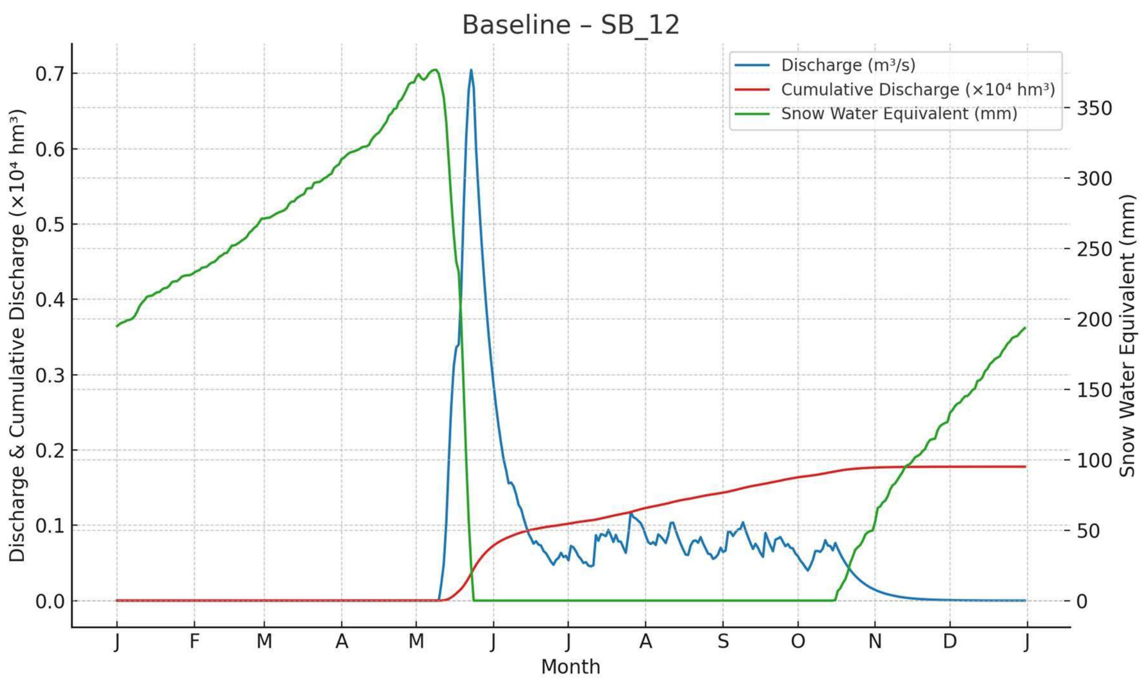

Figure 2-8: Baseline Hydrographs (SB_12)

2.2 Operation Scenarios

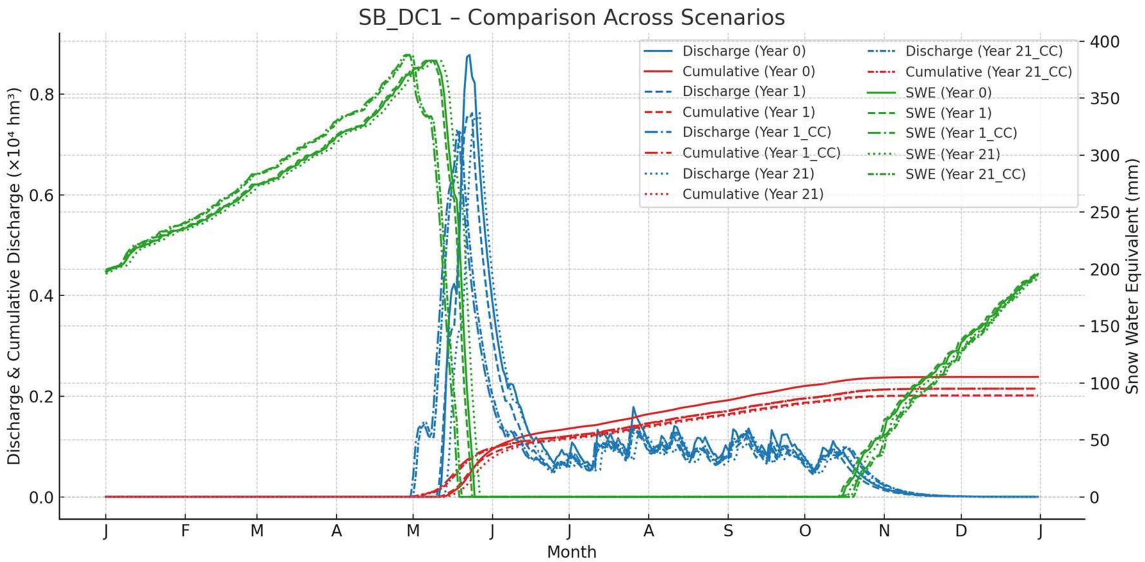

Figure 2-9: Operation and Construction Hydrographs (SB_DC1)

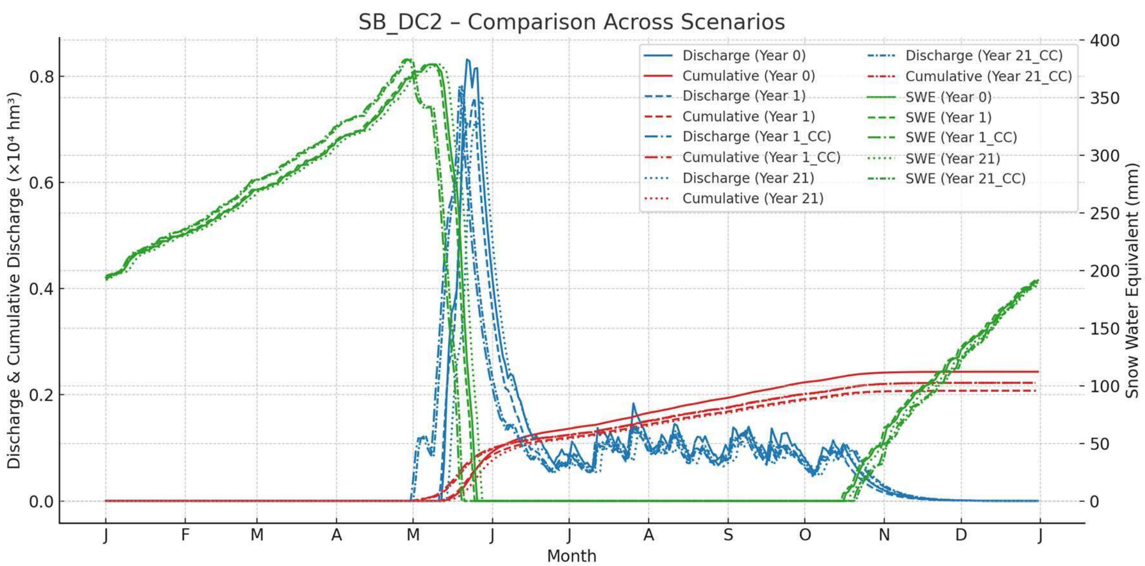

Figure 2-10: Operation and Construction Hydrographs (SB_DC2)

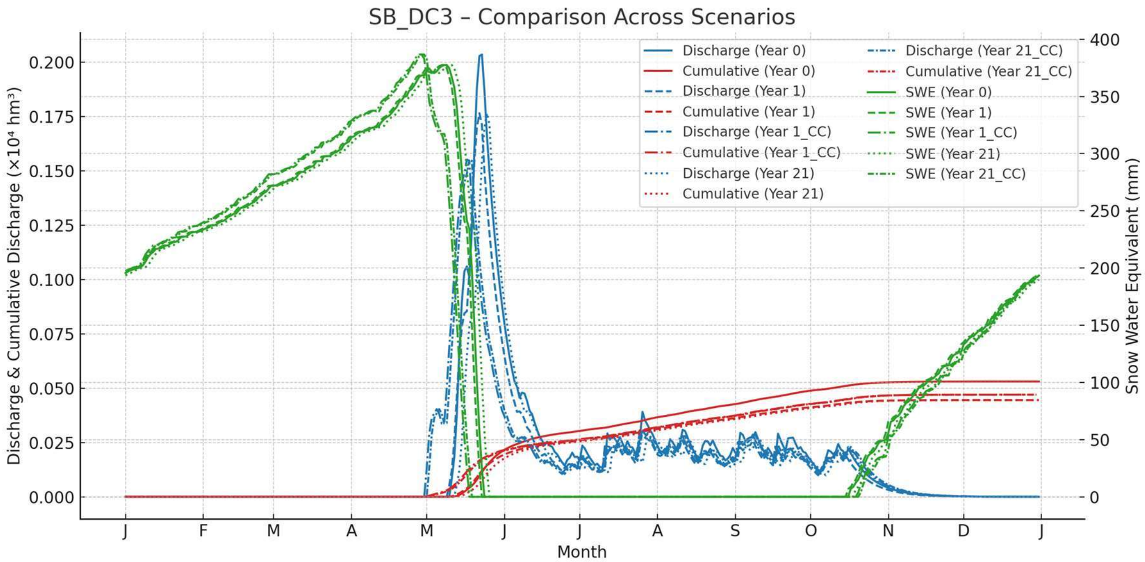

Figure 2-11: Operation and Construction Hydrographs (SB_DC3)

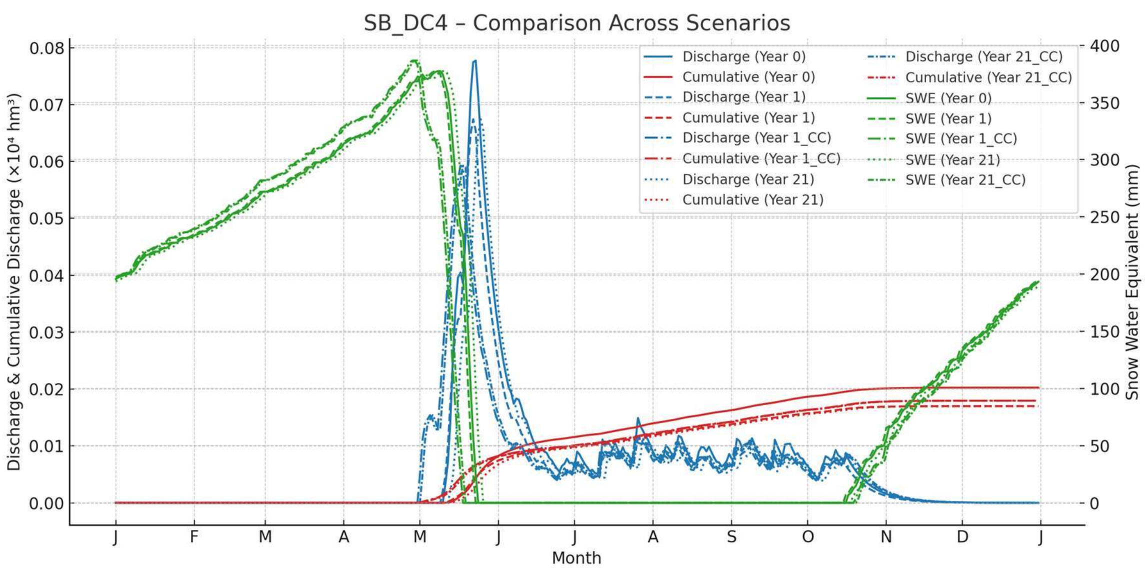

Figure 2-12: Operation and Construction Hydrographs (SB_DC4)

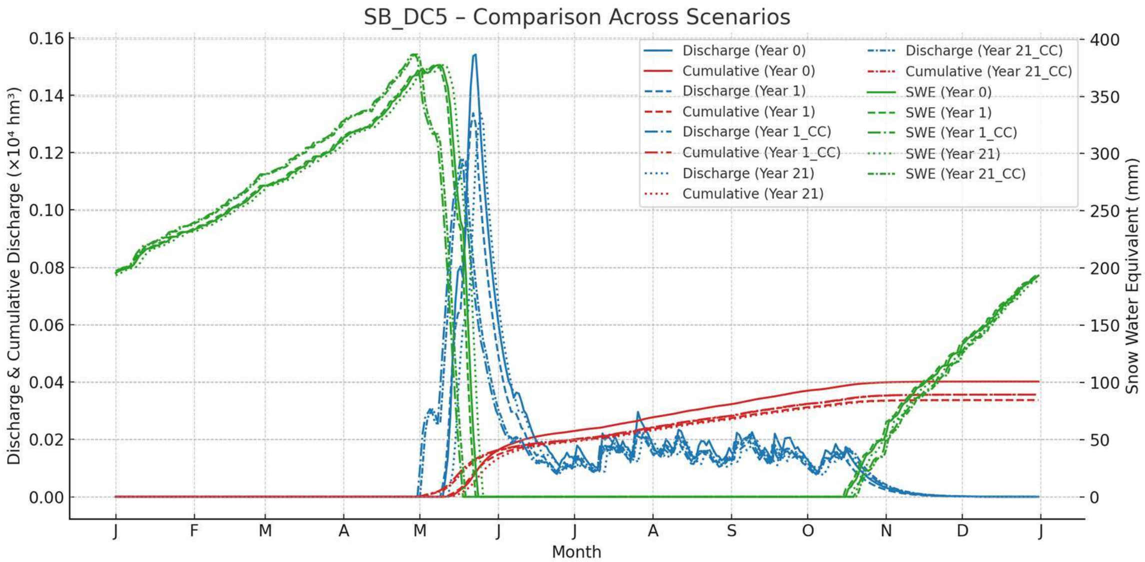

Figure 2-13: Operation and Construction Hydrographs (SB_DC5)

2.3 Sediment Ponds

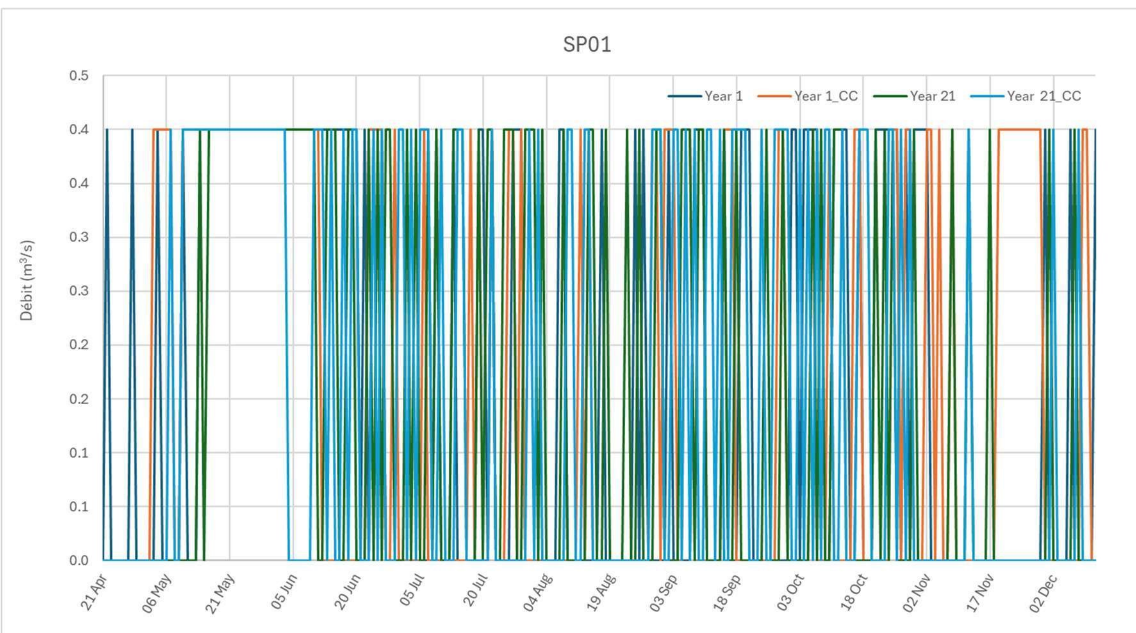

Figure 2-14: Sediment Pond Discharge (SP01)

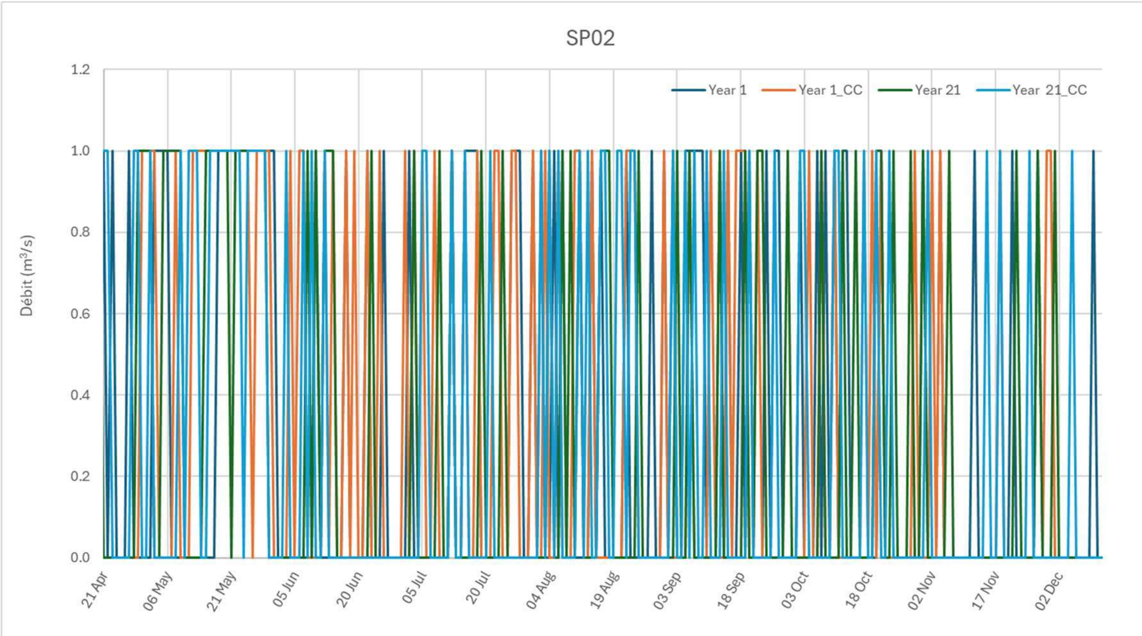

Figure 2-15: Sediment Pond Discharge (SP02)

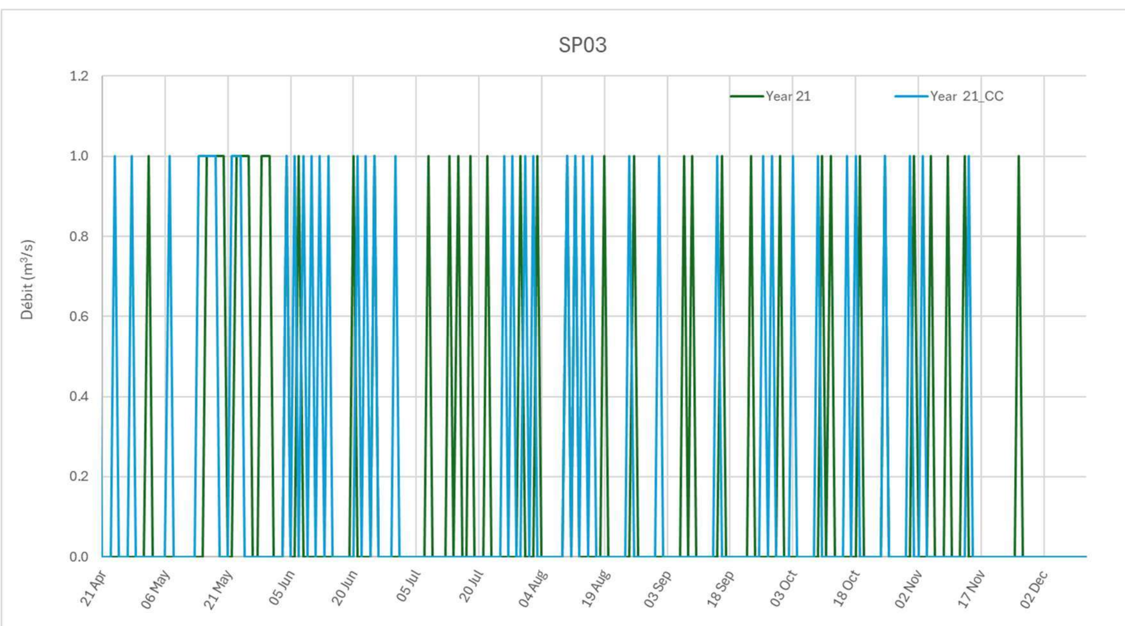

Figure 2-16: Sediment Pond Discharge (SP03)

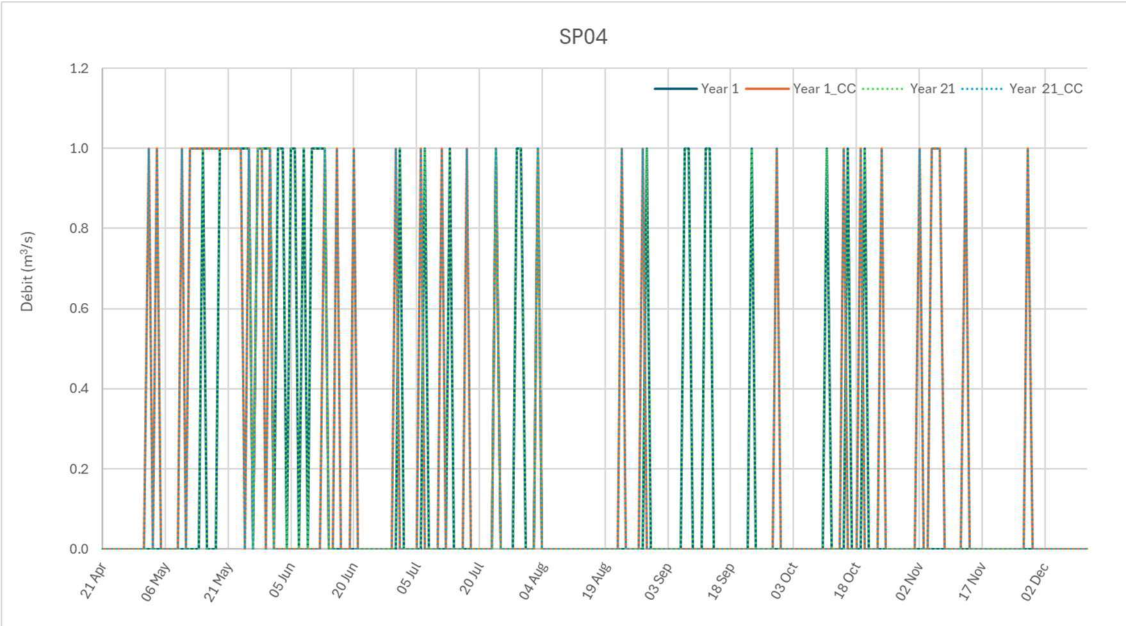

Figure 2-17: Sediment Pond Discharge (SP04)

2.4 Storage-Elevation Lake A

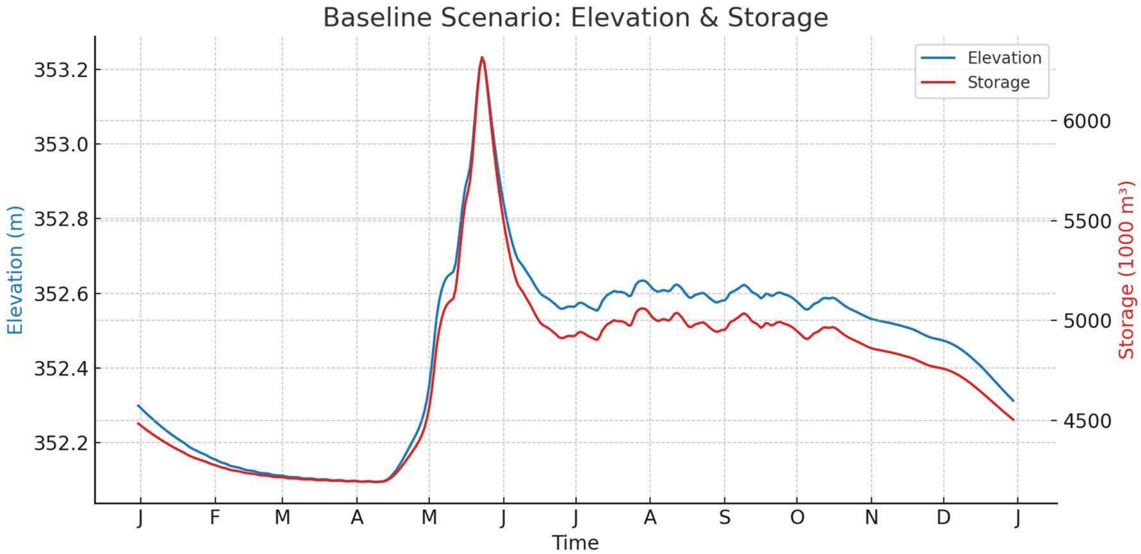

Figure 2-18: Storage-Elevation Lake A (Baseline)

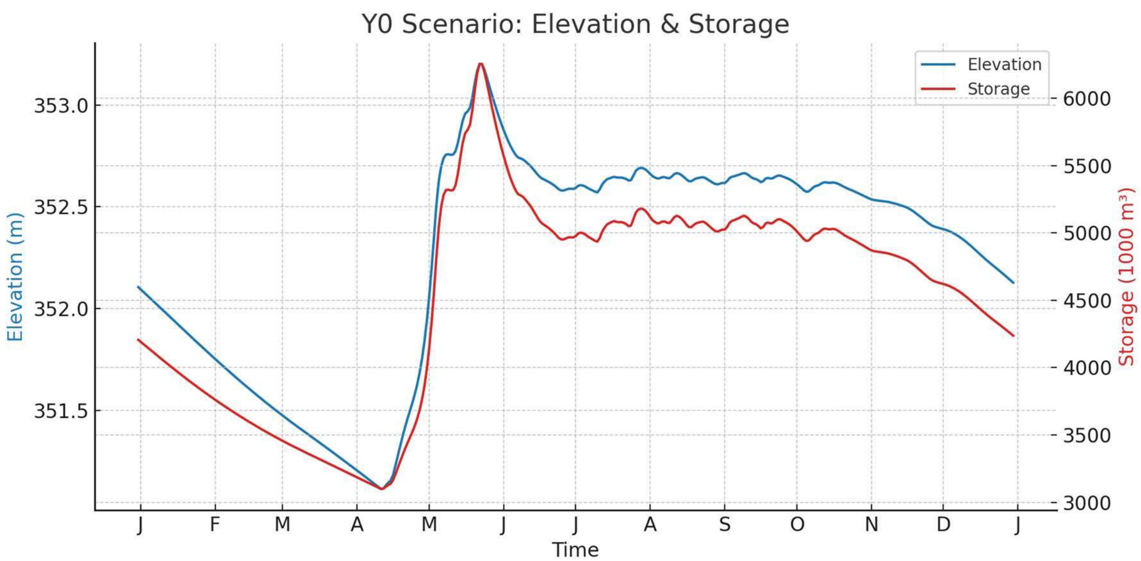

Figure 2-19: Storage-Elevation Lake A (End of Construction)

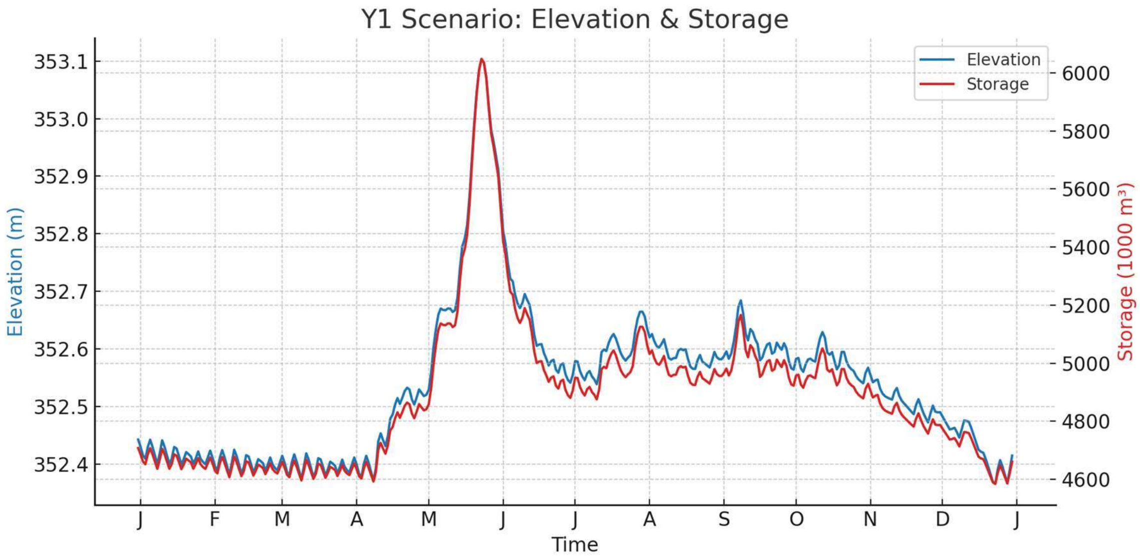

Figure 2-20: Storage-Elevation Lake A (Year 1 of Operation)

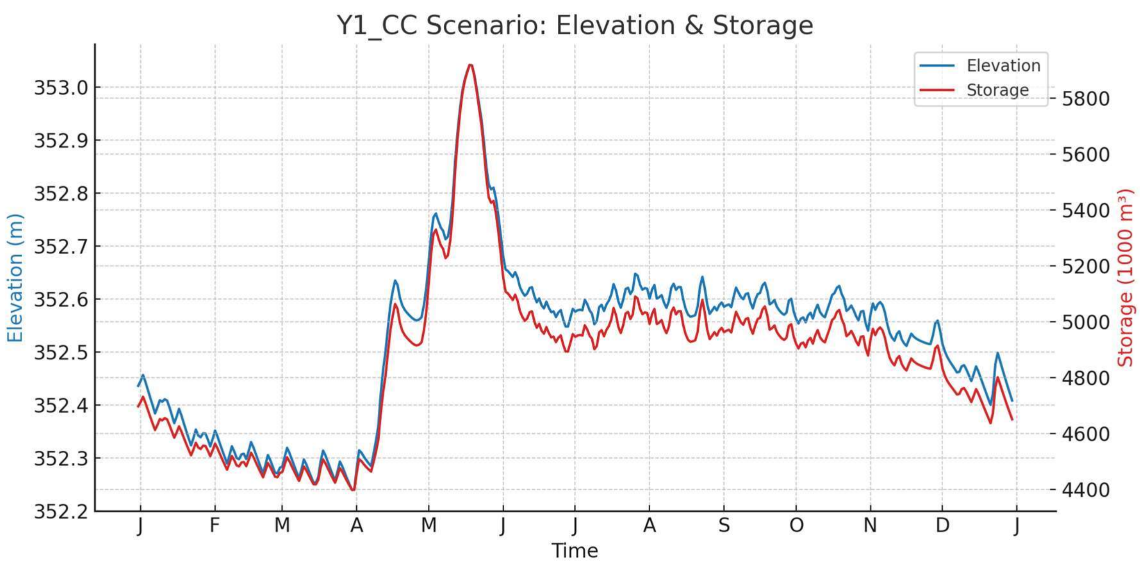

Figure 2-21: Storage-Elevation Lake A (Year 1 of Operation- Climate Change)

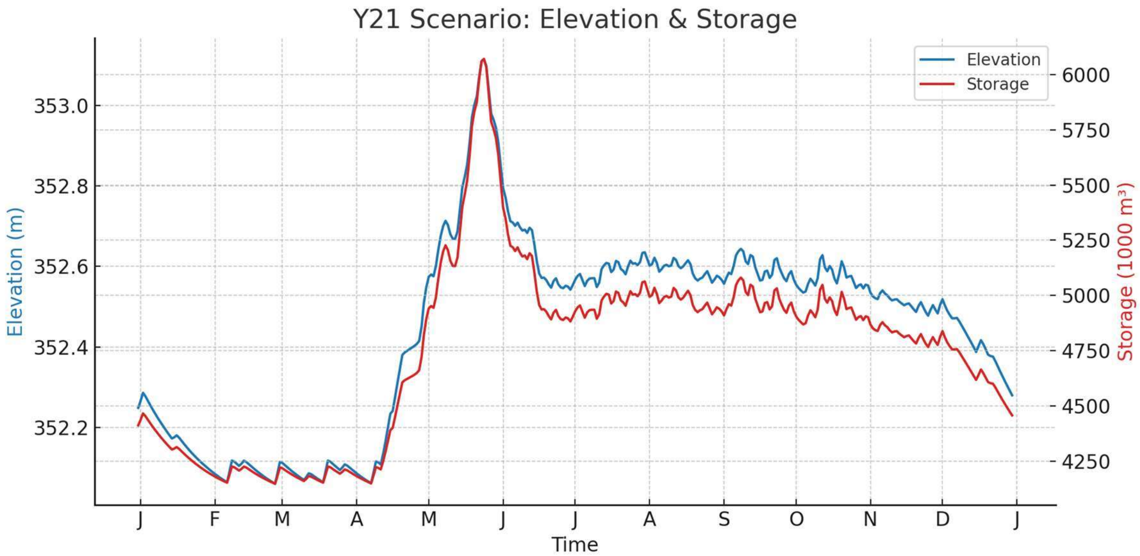

Figure 2-22: Storage-Elevation Lake A (Year 21 of Operation)

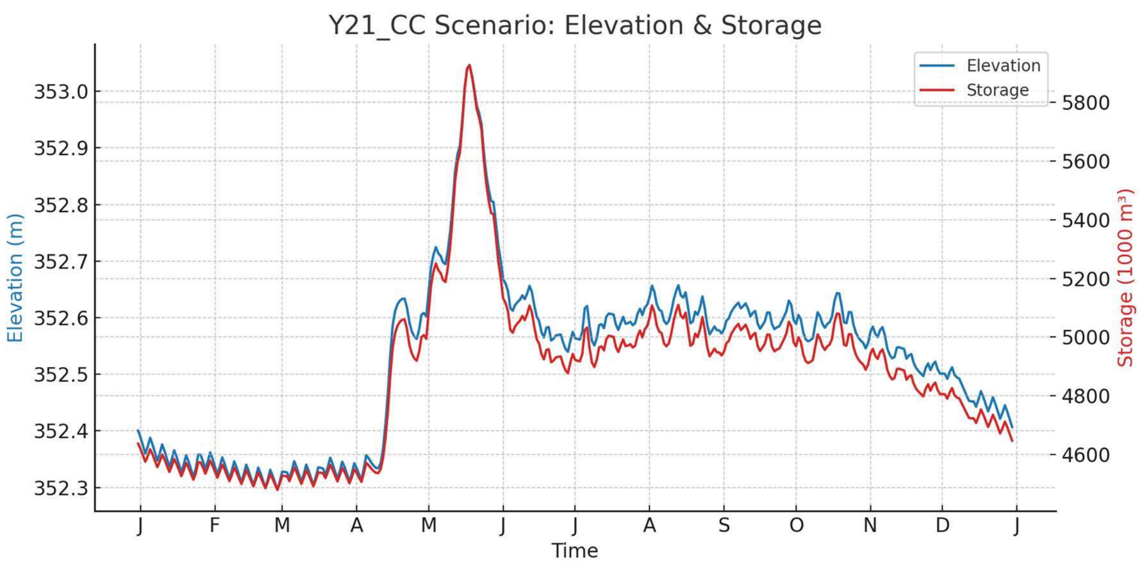

Figure 2-23: Storage-Elevation Lake A (Year 21 of Operation- Climate Change)

Appendix II

Summary Tables

3 Summary Tables

Table 3-1: Summary of hydrological elements for (Baseline Scenario), NA: Not Applicable

Hydrologic Element	Drainage Area (km^2)	Peak Discharge (m^3/s)	Volume (mm)
SB_TSF	5.7	2.3	1743.47
TSF Pond	5.7	2.3	1743.47
SB_02	4.7	1.2	1918.49
SB_01	10.4	2.6	1908.84
Source-GW2LacAmont	NA	0	NA
Lac Amont	NA	3	NA
bibou1	NA	3	NA
Junction 1	NA	3	NA
bibou1-DS-0	NA	3	NA
Junction 2	NA	3.6	NA
bibou1-DS-1	NA	3.6	NA
12-Jun	NA	4.6	NA
bibou2-DS-5	NA	4.6	NA
Sond 2a	NA	4.6	NA
bibou2-DS-0	NA	4.6	NA
4-Jun	NA	5.6	NA
bibou2-DS-1	NA	5.6	NA
5-Jun	NA	6.1	NA
bibou2-DS-2	NA	6.1	NA
13-Jun	NA	6.1	NA
bibou2-DS-6	NA	6.1	NA
6-Jun	NA	6.4	NA
bibou2-DS-3	NA	6.4	NA
SB_12	1.7	0.7	1800.42
11-Jun		7.1	
SB_13	1	0.4	1832.52
SB_23	1.6	0.6	1727.5
15-Jun	1.6	0.6	1727.5
17-Jun	4.4	1.8	1767.39
Reach-14-DS-1	4.4	1.8	1765.06
SB_19	2.8	1.1	1696.79
9-Jun	7.2	2.9	1738.77
Reach-13	7.2	2.9	1738.81
10-Jun	11.7	4.8	1751.04

Hydrologic Element	Drainage Area (km^2)	Peak Discharge (m^3/s)	Volume (mm)
Reach-11	11.7	4.8	1749.11
20-Jun	11.7	4.8	1749.11
SB_22	0.2	0.1	2086.28
2-Jun	0.2	0.1	2086.28
16-Jun	2.9	1.2	1789.38
Reach-14-DS-0	2.9	1.2	1789.38
SB_21	2.6	1.1	1764.77
18-Jun	2.6	1.1	1764.77
Reach-14-DS-2	2.6	1.1	1763.78
SB_16	3.7	1.5	1748.83
SB_17	0.8	0.3	1876.34
Reach-10	0	0	
8-Jun	0.6	0.2	1690.95
SB_18	1.1	0.4	1774.85
Reach-10-DS-0	0.6	0.2	1688.77
19-Jun	1.6	0.7	1744
SB_20	0.6	0.2	1690.95
14-Jun	1	0.4	1832.52
SB_14	0.6	0.2	1895.44
SB_15	0.6	0.3	1889.01
Source-GW2LacA	NA	0	NA
Outlet_lac A	NA	12.8	NA
SB_03	3.3	1.4	1824.45
Lac A	NA	12.8	NA
Reach-6	NA	0	NA
1-Jun	1.4	0.6	1819.95
Reach-5	1.4	0.6	1817.34
SB_06	1.4	0.6	1819.95
SB_05	0.7	0.3	1914.15
bibou2	0	0	NA
7-Jun	2.5	1	1806.83
bibou2-DS-4	2.5	1	1805.84
SB_04	2.5	1	1806.83
SB_09	2	0.8	1797.01
3-Jun	2	0.8	1797.01
Reach-2	2	0.8	1794.07
SB_08	0.4	0.2	1976.49
SB_07	1.2	0.5	1851.98

Hydrologic Element	Drainage Area (km^2)	Peak Discharge (m^3/s)	Volume (mm)
Reach-1	0	0	NA
Junction 3	0	0	NA
Reach-1-DS-0	0	0	NA
Reach-3	0	0	NA
SB_10	0.8	0.3	1826.54
SB_25	9.9	4.1	1779.94
SB_26	6.6	2.7	1784.1
Junc-26	NA	19.4	NA
SB_27	1.8	0.7	1818.26
SB_28	254.5	77.4	1572.67
Junc-27	NA	20.1	NA
Outlet	NA	97.5	NA
SInk TSF	5.7	2.3	1743.47
SB_Pit87	2.5	1	1795.41
Pit 87	2.8	1.1	1813.42
Sink Pit 87	2.8	1.1	1813.42
SB_24	0.3	0.1	1949.62
PitJ	0	0	NA
Sink Pit J	1.3	0.5	1801.1
SB_PitJ	1.3	0.5	1801.1
SB_11	0.1	0.1	2301.46
Polishing Pond	0	0	NA

Table 3-2: Summary of hydrological elements (End of Construction -Y0 Scenario), NA: Not Applicable

Hydrologic Element	Drainage Area (km^2)	Peak Discharge (m^3/s)	Volume (mm)
SB_S07	0.5	0.2	1912.46
S07	0.5	0.2	2463.75
SB_D04	0.1	0.1	2545.04
D04	0.1	0.1	2545.04
SB_S03	0.3	0.1	2075.32
SB_TSF	4.7	3.1	5475.66
S03	0.5	0.3	3788.97
SB_D03	0.1	0.1	2881.21
D03	0.1	0.1	2881.21
SB_S02	0	0.1	5440.08

Hydrologic Element	Drainage Area (km^2)	Peak Discharge (m^3/s)	Volume (mm)
S02	0.1	0.3	4393.22
SB_01	10.4	2.6	1909.36
SB_02	4.7	1.2	1919.01
Lac Amont	15.1	3.3	1925.84
7-Jun	15.1	3.3	1925.84
RDC0	15.1	3.3	1925.86
SB_DC_Outlet	0.3	0.1	2163.66
1-Jun	15.4	3.3	1929.91
RDC1	15.4	3.3	1928.87
SB_D01a	0.5	0.2	2022.71
D01a	0.5	0.2	2022.71
SB_D01b	0.2	0.1	2324.29
D01b	0.2	0.1	2324.29
AUX_01b_01c	0.6	0.3	2114.7
R_D01c	0.6	0.3	2114.8
SB_D01c	0.1	0.1	3392.06
D01c	0.7	0.3	2210.24
SB_D02	0.6	0.2	1958.55
D02	0.6	0.2	1958.55
SB_S01	0.1	0.1	2570.75
S01	1.4	0.2	2054.62
SB_D05	0.8	0.3	1897.68
D05	0.8	0.3	1897.68
SB_SP01	0.1	0.1	2496.41
SP01	2.4	0.4	2556.32
SB_DC_1	1.9	0.8	1891.93
WTP	NA	0	NA
2-Jun	NA	3.3	NA
RDC1-DS-0	NA	3.3	NA
8-Jun	0	0	NA
DCB	0	0	NA
SB_D17	2.1	0.6	1924.27
D17	2.1	0.6	1924.27
SB_D12	0.1	0.1	2501.37
D12	0.1	0.1	2501.37
SB_S06	0.6	0.3	2049.54
S06	0.7	0.2	2420.17
SB_D06b	0.3	0.1	2130.54

Hydrologic Element	Drainage Area (km^2)	Peak Discharge (m^3/s)	Volume (mm)
D06b	1.1	0.3	2331.89
SB_D06a	0.3	0.1	2116.99
D06a	0.3	0.1	2116.99
AUX_06a_06b	1.4	0.5	2282.03
R_D06c	1.4	0.5	2282.05
SB_D06c	0.1	0.1	2481.4
D06c	1.5	0.5	2300
9-Jun	2.1	0.6	1924.27
SB_SP02	0.1	0.1	2593.47
SP02	3.8	1	2521.09
SB_DC_2	2	0.8	1896.79
3-Jun	NA	4.3	NA
RDC1-DS-1	NA	4.3	NA
SB_DC_3	0.4	0.2	2054.72
4-Jun	NA	4.5	NA
RDC1-DS-2	NA	4.5	NA
SB_DC4	0.2	0.1	2367.57
5-Jun	NA	4.5	NA
RDC1-DS-3	NA	4.5	NA
SB_DC_5	0.3	0.1	2116.56
6-Jun	NA	4.7	NA
SB_DC2a	1.3	0.5	1816.25
DC2a	1.3	0.5	1816.25
SB_DC2b	4.3	1.7	1760.57
Sub-1	3.7	1.5	1583.1
Junc-1	9.3	3.7	1696.77
SB_D16	0.1	0.1	2515.63
SB_D14a	1.2	0.5	1883.03
D14a	1.2	0.5	1883.03
SB_S09	0.5	0.2	2095.84
S09	0.5	0.3	2011.08
SB_D14b	0.4	0.2	2134.03
D14b	0.9	0.5	2069.61
AUX_14a_14b	2.1	0.9	1961.33
R_D14c	2.1	0.9	1961.33
SB_D14c	0.2	0.1	2287.58
D14c	2.2	1	1987.69
SB_D15	0.4	0.1	2065.99

Hydrologic Element	Drainage Area (km^2)	Peak Discharge (m^3/s)	Volume (mm)
D15	0.4	0.1	2065.99
SB_SP04	0.2	0.1	2425.87
SP04	2.8	1	2192.58
R_D16	2.8	1	2192.58
D16	0.1	0.1	2515.63
Outlet_SP04	2.9	1.1	2205.49
SB_D11	0.8	0.3	1936.54
D11	0.8	0.3	1936.54
SB_D10a	0.5	0.2	2024.21
D10a	0.5	0.2	2024.21
SB_D10b	0.2	0.1	2260.71
D10b	0.2	0.1	2260.71
SB_SP03	0	0.1	3664.43
SP03	1.5	0.6	2063.74
RD18	1.5	0.6	2061.43
D18	1.5	0.6	2061.43
Sub-4	0.6	0.2	1808.73
Sub-3	0.6	0.2	1738.34
Lac A	NA	10.4	NA
Outlet_lacA	NA	10.4	NA
SB_25	9.9	4.1	1819.83
SB_26	6.6	2.7	1823.99
Junc-26	NA	17.2	NA
SB_27	0.6	0.3	1905.22
Junc-27	NA	17.4	NA
Outlet	NA	17.4	NA
Sink_TSF	5.8	3.5	5057.56
SB_Pit87	2.3	1.5	5542.23
Sink_Pit87	2.3	1.5	5542.23
SB_D08	0.1	0.1	2867.97
D08	0.1	0.1	2867.97
SB_D09	0	0.1	3990.1
D09	0	0.1	3990.1
SB_S05	0	0.1	4538.94
S05	0.1	0.2	5061.58
SB_PitJ	2	1.3	5617.54
Sink_PitJ	2.1	1.3	5578.78
SB_D07b	0.1	0.1	2554.55

Hydrologic Element	Drainage Area (km²)	Peak Discharge (m³/s)	Volume (mm)
D07b	0.1	0.1	2554.55
R_D07c	0.1	0.1	2554.64
SB_D07c	0	0.1	3592.58
D07c	0.2	0.2	2841.59
SB_PitX22	1.2	0.8	5576.57
Sink_PitX22	1.3	0.8	5214.24
SB_PitSW	1.1	0.7	5578.66
Sink_PitSW	1.1	0.7	5578.66
Sink SP04	0	0	NA
Sink-AuxSP02	0	0	NA

Table 3-3: Summary of hydrological elements (Year 1 of Operation -Y1 Scenario), NA: Not Applicable

Hydrologic Element	Drainage Area (km²)	Peak Discharge (m³/s)	Volume (mm)
SB_S07	0.5	0.2	1912.46
S07	0.5	0.2	2463.75
SB_D04	0.1	0.1	2545.04
D04	0.1	0.1	2545.04
SB_S03	0.3	0.1	2075.32
Tailing Storage S03	NA	0	NA
SB_TSF	4.7	3.1	5475.66
S03	NA	0.3	NA
SB_D03	0.1	0.1	2881.21
D03	0.1	0.1	2881.21
SB_S02	0	0.1	5440.08
Tailing Storage S02	NA	0	NA
S02	NA	0.3	NA
SB_01	10.4	2.6	1909.36
SB_02	4.7	1.2	1919.01
Source-GW2LacAmont	NA	0	NA
Lac Amont	NA	3.3	NA
7-Jun	NA	3.3	NA
RDC0	NA	3.3	NA
SB_DC_Outlet	0.3	0.1	2163.66
1-Jun	NA	3.3	NA

Hydrologic Element	Drainage Area (km^2)	Peak Discharge (m^3/s)	Volume (mm)
RDC1	NA	3.3	NA
SB_D01a	0.5	0.2	2022.71
D01a	0.5	0.2	2022.71
SB_D01b	0.2	0.1	2324.29
D01b	0.2	0.1	2324.29
AUX_01b_01c	0.6	0.3	2114.7
R_D01c	0.6	0.3	2114.8
SB_D01c	0.1	0.1	3392.06
D01c	0.7	0.3	2210.24
SB_D02	0.6	0.2	1958.55
D02	0.6	0.2	1958.55
SB_S01	0.1	0.1	2570.75
S01	1.4	0.2	2054.62
SB_D05	0.8	0.3	1897.68
D05	0.8	0.3	1897.68
SB_SP01	0.1	0.1	2496.41
Source-PitSW	NA	0.1	NA
SP01	NA	0.4	NA
SB_DC_1	1.9	0.8	1891.93
WTP	NA	0	NA
2-Jun	NA	3.7	NA
RDC1-DS-0	NA	3.7	NA
8-Jun	NA	0	NA
DCB	NA	0	NA
SB_D17	2.1	0.6	1924.27
D17	2.1	0.6	1924.27
SB_D12	0.1	0.1	2501.37
D12	0.1	0.1	2501.37
SB_S06	0.6	0.3	2049.54
S06	0.7	0.2	2420.17
SB_D06b	0.3	0.1	2130.54
D06b	1.1	0.3	2331.89
SB_D06a	0.3	0.1	2116.99
D06a	0.3	0.1	2116.99
AUX_06a_06b	1.4	0.5	2282.03
R_D06c	1.4	0.5	2282.05
SB_D06c	0.1	0.1	2481.4
D06c	1.5	0.5	2300

Hydrologic Element	Drainage Area (km²)	Peak Discharge (m³/s)	Volume (mm)
9-Jun	2.1	0.6	1924.27
SB_SP02	0.1	0.1	2593.47
Source-Pit87	NA	0.1	NA
Source-PitJ	NA	0	NA
Tailing Storage SP02	NA	0	NA
SP02	NA	1	NA
SB_DC_2	2	0.8	1896.79
3-Jun	NA	4.3	NA
RDC1-DS-1	NA	4.3	NA
SB_DC_3	0.4	0.2	2054.72
4-Jun	NA	4.5	NA
RDC1-DS-2	NA	4.5	NA
SB_DC4	0.2	0.1	2367.57
5-Jun	NA	4.6	NA
RDC1-DS-3	NA	4.6	NA
SB_DC_5	0.3	0.1	2116.56
6-Jun	NA	4.7	NA
SB_DC2a	1.3	0.5	1816.25
DC2a	1.3	0.5	1816.25
SB_DC2b	4.3	1.7	1760.57
Sub-1	3.7	1.5	1583.1
Junc-1	9.3	3.7	1696.77
SB_D16	0.1	0.1	2515.63
SB_D14a	1.2	0.5	1883.03
D14a	1.2	0.5	1883.03
SB_S09	0.5	0.2	2095.84
S09	0.5	0.3	2011.08
SB_D14b	0.4	0.2	2134.03
D14b	0.9	0.5	2069.61
AUX_14a_14b	2.1	0.9	1961.33
R_D14c	2.1	0.9	1961.33
SB_D14c	0.2	0.1	2287.58
D14c	2.2	1	1987.69
SB_D15	0.4	0.1	2065.99
D15	0.4	0.1	2065.99
SB_SP04	0.2	0.1	2425.87
SP04	2.8	1	2192.58
R_D16	2.8	1	2192.58

Hydrologic Element	Drainage Area (km^2)	Peak Discharge (m^3/s)	Volume (mm)
D16	0.1	0.1	2515.63
Outlet_SP04	2.9	1.1	2205.49
SB_D11	0.8	0.3	1936.54
D11	0.8	0.3	1936.54
SB_D10a	0.5	0.2	2024.21
D10a	0.5	0.2	2024.21
SB_D10b	0.2	0.1	2260.71
D10b	0.2	0.1	2260.71
SB_SP03	0	0.1	3664.43
SP03	1.5	0.6	2063.74
RD18	1.5	0.6	2061.43
D18	1.5	0.6	2061.43
Sub-4	0.6	0.2	1808.73
Sub-3	0.6	0.2	1738.34
Source-GW2LacA	NA	0	NA
Lac A	NA	10.4	NA
Source-1	NA	0	NA
Sink_TSF	NA	3.6	NA
SB_Pit87	2.3	1.5	5542.23
Sink_Pit87	2.3	1.5	5542.23
SB_D08	0.1	0.1	2867.97
D08	0.1	0.1	2867.97
SB_D09	0	0.1	3990.1
D09	0	0.1	3990.1
SB_S05	0	0.1	4538.94
S05	0.1	0.2	5061.58
SB_PitJ	2	1.3	5617.54
Sink_PitJ	2.1	1.3	5578.78
SB_D07b	0.1	0.1	2554.55
D07b	0.1	0.1	2554.55
R_D07c	0.1	0.1	2554.64
SB_D07c	0	0.1	3592.58
D07c	0.2	0.2	2841.59
SB_PitX22	1.2	0.8	5576.57
Sink_PitX22	1.3	0.8	5214.24
SB_PitSW	1.1	0.7	5578.66
Sink_PitSW	1.1	0.7	5578.66
Sink SP02	0	0	NA

Hydrologic Element	Drainage Area (km^2)	Peak Discharge (m^3/s)	Volume (mm)
Sink-AuxSP02	0	0	NA
drawdown_lacA	0	0.1	NA

Table 3-4: Summary of hydrological elements (Year 1 of Operation Climate change -Y1-CC Scenario), NA: Not Applicable

Hydrologic Element	Drainage Area (km^2)	Peak Discharge (m^3/s)	Volume (mm)
SB_S07	0.5	0.2	2040.67
S07	0.5	0.2	2565
SB_D04	0.1	0.1	2671.46
D04	0.1	0.1	2671.46
SB_S03	0.3	0.1	2201.77
Tailing Storage S03	NA	0	NA
SB_TSF	4.7	2.4	6007.02
S03	NA	0.3	NA
SB_D03	0.1	0.1	3007.12
D03	0.1	0.1	3007.12
SB_S02	0	0.1	5564.18
Tailing Storage S02	NA	0	NA
S02	NA	0.3	NA
SB_01	10.4	2.3	2088.88
SB_02	4.7	1	2098.53
Source-GW2LacAmont	NA	0	NA
Lac Amont	NA	2.7	NA
7-Jun	NA	2.7	NA
RDC0	NA	2.7	NA
SB_DC_Outlet	0.3	0.1	2300.92
1-Jun	NA	2.7	NA
RDC1	NA	2.7	NA
SB_D01a	0.5	0.2	2150.53
D01a	0.5	0.2	2150.53
SB_D01b	0.2	0.1	2449.41
D01b	0.2	0.1	2449.41
AUX_01b_01c	0.6	0.2	2241.7
R_D01c	0.6	0.2	2241.79
SB_D01c	0.1	0.1	3520.28
D01c	0.7	0.3	2337.33

Hydrologic Element	Drainage Area (km^2)	Peak Discharge (m^3/s)	Volume (mm)
SB_D02	0.6	0.2	2087.07
D02	0.6	0.2	2087.07
SB_S01	0.1	0.1	2695.23
S01	1.4	0.2	2148.01
SB_D05	0.8	0.3	2036.11
D05	0.8	0.3	2036.11
SB_SP01	0.1	0.1	2620.96
Source-PitSW	NA	0.1	NA
SP01	NA	0.4	NA
SB_DC_1	1.9	0.7	2029.19
WTP	NA	0	NA
2-Jun	NA	3.2	NA
RDC1-DS-0	NA	3.2	NA
8-Jun	0	0	NA
DCB	0	0	NA
SB_D17	2.1	0.5	2044.96
D17	2.1	0.5	2044.96
SB_D12	0.1	0.1	2624.53
D12	0.1	0.1	2624.53
SB_S06	0.6	0.2	2173.21
S06	0.7	0.2	2558.46
SB_D06b	0.3	0.1	2255.26
D06b	1.1	0.3	2466.05
SB_D06a	0.3	0.1	2242.26
D06a	0.3	0.1	2242.26
AUX_06a_06b	1.4	0.4	2414.12
R_D06c	1.4	0.4	2414.15
SB_D06c	0.1	0.1	2605.78
D06c	1.5	0.5	2431.4
9-Jun	2.1	0.5	2044.96
SB_SP02	0.1	0.1	2716.55
Source-Pit87	NA	0.1	NA
Source-PitJ	NA	0	NA
Tailing Storage SP02	NA	0	NA
SP02	NA	1	NA
SB_DC_2	2	0.8	2041.44
3-Jun	NA	3.9	NA
RDC1-DS-1	NA	3.9	NA

Hydrologic Element	Drainage Area (km^2)	Peak Discharge (m^3/s)	Volume (mm)
SB_DC_3	0.4	0.2	2179.97
4-Jun	NA	4	NA
RDC1-DS-2	NA	4	NA
SB_DC4	0.2	0.1	2492.82
5-Jun	NA	4.1	NA
RDC1-DS-3	NA	4.1	NA
SB_DC_5	0.3	0.1	2241.8
6-Jun	NA	4.2	NA
SB_DC2a	1.3	0.5	1944.5
DC2a	1.3	0.5	1944.5
SB_DC2b	4.3	1.5	1889
Sub-1	3.7	1.3	1712.53
Junc-1	9.3	3.3	1825.58
SB_D16	0.1	0.1	2642.77
SB_D14a	1.2	0.4	2009.85
D14a	1.2	0.4	2009.85
SB_S09	0.5	0.2	2219.52
S09	0.5	0.3	2987.9
SB_D14b	0.4	0.2	2257.19
D14b	0.9	0.5	2640.07
AUX_14a_14b	2.1	0.9	2274.33
R_D14c	2.1	0.9	2274.33
SB_D14c	0.2	0.1	2413.89
D14c	2.2	1	2285.6
SB_D15	0.4	0.1	2192.29
D15	0.4	0.1	2192.29
SB_SP04	0.2	0.1	2548.96
SP04	2.8	1	2912.99
R_D16	2.8	1	2912.99
D16	0.1	0.1	2642.77
Outlet_SP04	2.9	1.1	2902.19
SB_D11	0.8	0.3	2062.85
D11	0.8	0.3	2062.85
SB_D10a	0.5	0.2	2149.79
D10a	0.5	0.2	2149.79
SB_D10b	0.2	0.1	2384.73
D10b	0.2	0.1	2384.73
SB_SP03	0	0.1	3788.78

Hydrologic Element	Drainage Area (km^2)	Peak Discharge (m^3/s)	Volume (mm)
SP03	1.5	0.6	2189.43
RD18	1.5	0.6	2182.24
D18	1.5	0.6	2182.24
Sub-4	0.6	0.2	1936.99
Sub-3	0.6	0.2	1867.77
Source-GW2LacA	NA	0	NA
Lac A	NA	9.3	NA
Outlet_lacA	NA	9.3	NA
Source-1	NA	0	NA
SB_25	9.9	3.6	1908.58
SB_26	6.6	2.4	1912.74
Junc-26	NA	15.3	NA
SB_27	1.8	0.6	1946.9
Junc-27	NA	15.9	NA
Outlet	NA	15.9	NA
Sink_TSF	NA	2.9	NA
SB_Pit87	2.3	1.1	6099.64
Sink_Pit87	2.3	1.1	6099.64
SB_D08	0.1	0.1	2993.9
D08	0.1	0.1	2993.9
SB_D09	0	0.1	4118.83
D09	0	0.1	4118.83
SB_S05	0	0.1	4665.34
S05	0.1	0.2	3766.76
SB_PitJ	2	1.1	6147.02
Sink_PitJ	2.1	1.1	5981.08
SB_D07b	0.1	0.1	2678.13
D07b	0.1	0.1	2678.13
R_D07c	0.1	0.1	2678.23
SB_D07c	0	0.1	3716.05
D07c	0.2	0.2	2965.15
SB_PitX22	1.2	0.6	6133.98
Sink_PitX22	1.3	0.6	5714.18
SB_PitSW	1.1	0.6	6136.08
Sink_PitSW	1.1	0.6	6136.08
Sink SP04	0	0	NA
Sink-AuxSP02	0	0	NA
drawdown_LacA	0	0.1	NA

Table 3-5: Summary of hydrological elements (Year 21 of Operation -Y21 Scenario). NA: Not Applicable

Hydrologic Element	Drainage Area (km^2)	Peak Discharge (m^3/s)	Volume (mm)
SB_S07	0.5	0.2	1912.46
S07	0.5	0.2	2463.75
SB_TSF	4.7	3.1	5475.66
SB_01	10.4	2.6	1909.36
SB_02	4.7	1.2	1919.01
Source-GW2LacAmont	NA	0	NA
Lac Amont	NA	3.3	NA
7-Jun	NA	3.3	NA
RDC0	NA	3.3	NA
SB_DC_Outlet	0.3	0.1	2163.66
1-Jun	NA	3.3	NA
RDC1	NA	3.3	NA
SB_D02	0.6	0.2	1958.55
SB_D01a	0.5	0.2	2022.71
D01a	0.5	0.2	2022.71
R_D02	0.5	0.2	2022.79
D02	1	0.4	1987.06
SB_S01	0.1	0.1	2570.75
S01	1.1	0.2	2088.97
SB_D05	0.8	0.3	1897.68
D05	0.8	0.3	1897.68
SB_SP01	0.1	0.1	2496.41
Tailing Storage SP01	NA	0	NA
SP01	NA	0.4	NA
SB_DC_1	1.9	0.8	1891.93
WTP	NA	0	NA
2-Jun	NA	3.3	NA
RDC1-DS-0	NA	3.3	NA
8-Jun	0	0	NA
DCB	0	0	NA
SB_D17	2.1	0.6	1924.27
D17	2.1	0.6	1924.27
9-Jun	2.1	0.6	1924.27
SB_D12	0.1	0.1	2501.37

Hydrologic Element	Drainage Area (km^2)	Peak Discharge (m^3/s)	Volume (mm)
D12	0.1	0.1	2501.37
SB_S06	0.6	0.3	2049.54
S06	0.7	0.2	2420.17
SB_D06b	0.3	0.1	2130.54
D06b	1.1	0.3	2331.89
SB_D06a	0.3	0.1	2116.99
D06a	0.3	0.1	2116.99
AUX_06a_06b	1.4	0.5	2282.03
R_D06c	1.4	0.5	2282.05
SB_D06c	0.1	0.1	2481.4
D06c	1.5	0.5	2300
SB_SP02	0.1	0.1	2593.47
Tailing Storage SP02	NA	0	NA
Pit X22 SP02	NA	0	NA
SP02	NA	1	NA
SB_DC_2	2	0.8	1896.79
3-Jun	NA	4.3	NA
RDC1-DS-1	NA	4.3	NA
SB_DC_3	0.4	0.2	2054.72
4-Jun	NA	4.5	NA
RDC1-DS-2	NA	4.5	NA
SB_DC4	0.2	0.1	2367.57
5-Jun	NA	4.6	NA
RDC1-DS-3	NA	4.6	NA
SB_DC_5	0.3	0.1	2116.56
6-Jun	NA	4.7	NA
SB_DC2a	1.3	0.5	1816.25
DC2a	1.3	0.5	1816.25
SB_DC2b	4.3	1.7	1760.57
Sub-1	3.7	1.5	1583.1
Junc-1	9.3	3.7	1696.77
SB_D16	0.1	0.1	2515.63
SB_D14a	1.2	0.5	1883.03
D14a	1.2	0.5	1883.03
SB_S09	0.5	0.2	2095.84
S09	0.5	0.3	2011.08
SB_D14b	0.4	0.2	2134.03
D14b	0.9	0.5	2069.61

Hydrologic Element	Drainage Area (km^2)	Peak Discharge (m^3/s)	Volume (mm)
AUX_14a_14b	2.1	0.9	1961.33
R_D14c	2.1	0.9	1961.33
SB_D14c	0.2	0.1	2287.58
D14c	2.2	1	1987.69
SB_D15	0.4	0.1	2065.99
D15	0.4	0.1	2065.99
SB_SP04	0.2	0.1	2425.87
SP04	2.8	1	2192.58
R_D16	2.8	1	2192.58
D16	0.1	0.1	2515.63
Outlet_SP04	2.9	1.1	2205.49
SB_D11	0.8	0.3	1936.54
D11	0.8	0.3	1936.54
SB_D10a	0.5	0.2	2024.21
D10a	0.5	0.2	2024.21
SB_D10b	0.2	0.1	2260.71
D10b	0.2	0.1	2260.71
SB_D08	0.1	0.1	2867.97
D08	0.1	0.1	2867.97
SB_D09	0	0.1	3990.1
D09	0	0.1	3990.1
SB_S05	0	0.1	4538.94
S05	0.1	0.2	5061.58
SB_SP03	0	0.1	3664.43
Source Pit J	NA	0.1	NA
SP03	NA	1	NA
RD18	NA	1	NA
D18	NA	1	NA
Sub-4	0.6	0.2	1808.73
Sub-3	0.6	0.2	1738.34
Source-GW2LacA	NA	0	NA
Lac A	NA	10.3	NA
Outlet_lacA	NA	10.3	NA
SB_25	9.9	4.1	1780.76
SB_26	6.6	2.7	1784.92
Junc-26	NA	17	NA
SB_27	1.8	0.7	1819.08
Junc-27	NA	17.8	NA

Hydrologic Element	Drainage Area (km^2)	Peak Discharge (m^3/s)	Volume (mm)
Outlet	NA	17.8	NA
Sink_TSF	5.2	3.3	5180.63
SB_Pit87	2.3	1.5	5542.23
Sink_Pit87	2.3	1.5	5542.23
SB_PitJ	2	1.3	5617.54
Sink_PitJ	2	1.3	5617.54
SB_D07b	0.1	0.1	2554.55
D07b	0.1	0.1	2554.55
R_D07c	0.1	0.1	2554.64
SB_D07c	0	0.1	3592.58
D07c	0.2	0.2	2841.59
SB_PitX22	1.2	0.8	5576.57
Sink_PitX22	1.3	0.8	5214.24
Sink SP04	NA	NA	NA
Sink-AuxSP02	NA	NA	NA
TSF WTP	NA	0	NA
drawdown_lacA	NA	0.1	NA

Table 3-6: Summary of hydrological elements (Year 21 of Operation Climate change -Y21-CC Scenario), NA: Not Applicable

Hydrologic Element	Drainage Area (KM2)	Peak Discharge (M3/s)	Volume (MM)
SB_S07	0.5	0.2	2040.67
S07	0.5	0.2	2565
SB_TSF	4.7	2.4	6007.02
SB_01	10.4	2.3	2088.88
SB_02	4.7	1	2098.53
Source-GW2LacAmont	NA	0	NA
Lac Amont	NA	2.7	NA
7-Jun	NA	2.7	NA
RDC0	NA	2.7	NA
SB_DC_Outlet	0.3	0.1	2300.92
1-Jun	NA	2.7	NA
RDC1	NA	2.7	NA
SB_D02	0.6	0.2	2087.07
SB_D01a	0.5	0.2	2150.53
D01a	0.5	0.2	2150.53

Hydrologic Element	Drainage Area (KM2)	Peak Discharge (M3/s)	Volume (MM)
R_D02	0.5	0.2	2150.61
D02	1	0.4	2115.27
SB_S01	0.1	0.1	2695.23
S01	1.1	0.2	2373.84
SB_D05	0.8	0.3	2036.11
D05	0.8	0.3	2036.11
SB_SP01	0.1	0.1	2620.96
Tailing Storage SP01	NA	0	NA
SP01	NA	0.4	NA
SB_DC_1	1.9	0.7	2029.19
WTP	NA	0.1	NA
2-Jun	NA	2.8	NA
RDC1-DS-0	NA	2.8	NA
8-Jun	NA	0	NA
DCB	NA	0	NA
SB_D17	2.1	0.5	2044.96
D17	2.1	0.5	2044.96
9-Jun	2.1	0.5	2044.96
SB_D12	0.1	0.1	2624.53
D12	0.1	0.1	2624.53
SB_S06	0.6	0.2	2173.21
S06	0.7	0.2	2558.46
SB_D06b	0.3	0.1	2255.26
D06b	1.1	0.3	2466.05
SB_D06a	0.3	0.1	2242.26
D06a	0.3	0.1	2242.26
AUX_06a_06b	1.4	0.4	2414.12
R_D06c	1.4	0.4	2414.15
SB_D06c	0.1	0.1	2605.78
D06c	1.5	0.5	2431.4
SB_SP02	0.1	0.1	2716.55
Tailing Storage SP02	NA	0	NA
Pit X22 SP02	NA	0	NA
SP02	NA	1	NA
SB_DC_2	2	0.8	2041.44
3-Jun	NA	3.9	NA
RDC1-DS-1	NA	3.9	NA
SB_DC_3	0.4	0.2	2179.97

Hydrologic Element	Drainage Area (KM2)	Peak Discharge (M3/s)	Volume (MM)
4-Jun	NA	4.1	NA
RDC1-DS-2	NA	4.1	NA
SB_DC4	0.2	0.1	2492.82
5-Jun	NA	4.1	NA
RDC1-DS-3	NA	4.1	NA
SB_DC_5	0.3	0.1	2241.8
6-Jun	NA	4.2	NA
SB_DC2a	1.3	0.5	1944.5
DC2a	1.3	0.5	1944.5
SB_DC2b	4.3	1.5	1889
Sub-1	3.7	1.3	1712.53
Junc-1	9.3	3.3	1825.58
SB_D16	0.1	0.1	2642.77
SB_D14a	1.2	0.4	2009.85
D14a	1.2	0.4	2009.85
SB_S09	0.5	0.2	2219.52
S09	0.5	0.3	2987.9
SB_D14b	0.4	0.2	2257.19
D14b	0.9	0.5	2640.07
AUX_14a_14b	2.1	0.9	2274.33
R_D14c	2.1	0.9	2274.33
SB_D14c	0.2	0.1	2413.89
D14c	2.2	1	2285.6
SB_D15	0.4	0.1	2192.29
D15	0.4	0.1	2192.29
SB_SP04	0.2	0.1	2548.96
SP04	2.8	1	2912.99
R_D16	2.8	1	2912.99
D16	0.1	0.1	2642.77
Outlet_SP04	2.9	1.1	2902.19
SB_D11	0.8	0.3	2062.85
D11	0.8	0.3	2062.85
SB_D10a	0.5	0.2	2149.79
D10a	0.5	0.2	2149.79
SB_D10b	0.2	0.1	2384.73
D10b	0.2	0.1	2384.73
SB_D08	0.1	0.1	2993.9
D08	0.1	0.1	2993.9

Hydrologic Element	Drainage Area (KM2)	Peak Discharge (M3/s)	Volume (MM)
SB_D09	0	0.1	4118.83
D09	0	0.1	4118.83
SB_S05	0	0.1	4665.34
S05	0.1	0.2	3766.76
SB_SP03	0	0.1	3788.78
Source Pit J	NA	0.1	NA
SP03	NA	0	NA
RD18	NA	0	NA
D18	NA	0	NA
Sub-4	0.6	0.2	1936.99
Sub-3	0.6	0.2	1867.77
Source-GW2LacA	NA	0	NA
Lac A	NA	8.6	NA
Outlet_lacA	NA	8.6	NA
SB_25	9.9	3.6	1908.58
SB_26	6.6	2.4	1912.74
Junc-26	NA	14.2	NA
SB_27	NA	0.6	NA
SB_28	254.5	72.3	1711.11
Junc-27	NA	14.9	NA
Outlet	NA	87.2	NA
Sink_TSF	5.2	2.6	5669.87
SB_Pit87	2.3	1.1	6099.64
Sink_Pit87	2.3	1.1	6099.64
SB_PitJ	2	1.1	6147.02
Sink_PitJ	2	1.1	6147.02
SB_D07b	0.1	0.1	2678.13
D07b	0.1	0.1	2678.13
R_D07c	0.1	0.1	2678.23
SB_D07c	0	0.1	3716.05
D07c	0.2	0.2	2965.15
SB_PitX22	1.2	0.6	6133.98
Sink_PitX22	1.3	0.6	5714.18
Sink SP04	NA	0	NA
Sink-AuxSP02	NA	0	NA
drawdown_lacA	NA	0.1	NA

1682 Woodward Dr.
Ottawa, ON K2C 3R8
Canada

T 877.487.8436
Ottawa@blumetric.ca

The Tower, 4 Cataraqui St.
Kingston, ON K7K 1Z7
Canada

T 877.487.8436
Kingston@blumetric.ca

3B-209 Frederick St.
Kitchener, ON N2H 2M7
Canada

T 877.487.8436
Kitchener@blumetric.ca

825 Milner Ave.
Toronto, ON M1B 3C3
Canada

T 877.487.8436
Toronto@blumetric.ca

6-410 Falconbridge Rd.
Sudbury, ON P3A 4S4
Canada

T 877.487.8436
Sudbury@blumetric.ca

260-15 Taschereau St.
Gatineau, QC J8Y 2V6
Canada

T 877.487.8436
Gatineau@blumetric.ca

200-1500 Du College St.
Saint-Laurent, QC H4L 5G6
Canada

T 877.487.8436
Montreal@blumetric.ca

27 Parker St.
Dartmouth, NS B2Y 4T5
Canada

T 877.487.8436
Dartmouth@blumetric.ca

4916 49th St.
Yellowknife, NT X1A 1P3
Canada

T 877.487.8436
Yellowknife@blumetric.ca

200-4445 SW 35th Terrace
Gainesville, FL 32608
USA

T 877.487.8436
Gainesville@blumetric.ca